AN ISOTOPE HYDROLOGY STUDY OF THE KILAUEA VOLCANO AREA, HAWAII

M.A. Scholl, S.E. Ingebritsen, C.J. Janik, and J.P. Kauahikaua

U.S. GEOLOGICAL SURVEY

Water-Resources Investigations Report 95-4213

Menlo Park, California
1995

DEPARTMENT OF THE INTERIOR
BRUCE BABBITT, Secretary
U.S. GEOLOGICAL SURVEY
Gordon P. Eaton, Director

The use of product names in this report is for descriptive purposes only and does not constitute endorsement of products by the U.S. Government.

For additional information
write to:

Chief, Branch of Regional Research
Water Resources Division
U.S. Geological Survey
345 Middlefield Road
Menlo Park, California
94025

Copies of this report
can be purchased from:

U.S. Geological Survey
Earth Science Information Center
Open-File Reports Services
Box 25286, MS 517
Federal Center
Denver, Colorado, 80225-0046

CONTENTS

ABSTRACT 1

INTRODUCTION 1
- Purpose and Scope 1
- Geologic Structure as Related to Hydrology 3
- Occurrence of Ground Water 3
- Climate and Rainfall 4
- Mechanisms for Differences in Rainfall Isotopic Composition 6
- Previous Isotopic Studies 7
- Acknowledgments 8

SAMPLE COLLECTION METHODS 8
- Precipitation 8
- Ground Water 10

INTERPRETATION OF STABLE ISOTOPE AND TRITIUM DATA 11
- Stable Isotope Composition of Rainfall 11
- Seasonal Variations in Stable Isotopes in Precipitation 11
- Throughfall 13
- Relation Between Rainfall Stable Isotope Composition and Elevation 14
- Stable Isotope Composition of Ground Water 18
- Estimation of Recharge Elevations 19
- Tritium 23

INTERPRETATION OF GROUND-WATER HYDROLOGY 25
- General Considerations in Interpretation of Ground-water Samples 25
- Compartmentalization of Regional Ground-water System by Rift Zones 26
  - West of Kilauea's Southwest Rift Zone 26
  - South of Kilauea's summit and East Rift Zone 26
  - North of Kilauea's East Rift Zone 28
  - Compartmentalization by Rift Zones 28
- Down-rift Ground-water Flow: SWRZ Versus ERZ 29
- Isotopic Enrichment in Thermal Waters 31

SUMMARY 32

REFERENCES 33

ILLUSTRATIONS

Figure 1. Map Showing Location of the Study Area in the Southeast Part of the Island of Hawaii 2

2. Map Showing Median Annual Rainfall in the Study Area 5

3. Daily Rainfall During the Study Period for the Tradewind and Rain Shadow Areas 6

4. Map Showing Location of Precipitation and Ground-water Sample Sites 9

5. Graphs Showing Relation of δD and $\delta^{18}O$ in Precipitation for Each Six-Month Collection Period of the Study 12

6. Graph Showing Temporal Variation of $\delta^{18}O$ in Precipitation at Ten Sample Collection Sites 12

7. A. Map of Study Area, Showing Samples Used to Determine Relation Between Isotopic Content of Precipitation and Elevation 15

B. Relation Between Volume-Weighted Average $\delta^{18}O$ in Precipitation and Elevation of Sample Site 15

8. Graph Showing Relation of Precipitation Isotope Data to Processes Controlling Condensation from Oceanic Vapor 16

9. Relation Between δD and $\delta^{18}O$ in Ground-water Samples 19

10. Map Showing Relative Age of Water Discharging at Springs and Wells, Calculated from Tritium Measurements 23

11. Map Showing Estimated Recharge Elevations for Springs and Wells, Calculated from Stable Isotope Measurements 27

TABLES

Table 1. Comparison of Volume and Isotopic Composition of Precipitation in Open-Sky and Throughfall Duplicate Collectors 14

2. Recharge Elevation Estimates for Ground-water Sample Sites 21

3. Tritium Measured in Ground Water, with Age Estimates 24

APPENDIXES

Appendix:

1. Location, Amount and Isotopic Composition of Precipitation Collected During Study 38

2. Location, Chloride Content, and Isotopic Composition of Ground-water Samples Collected During Study 41

CONVERSION FACTORS

Multiply	by	To obtain
meter (m)	3.281	feet
square meter (m^2)	10.764	square feet
kilometer (km)	0.6214	mile
square kilometer (km^2)	0.3861	square mile
gram (g)	0.0353	ounce
liter (L)	0.2642	gallon

For conversion of degrees Celsius (°C) to degrees Fahrenheit (°F), use the formula:

$$°F = 1.8°C + 32$$

AN ISOTOPE HYDROLOGY STUDY OF THE KILAUEA VOLCANO AREA, HAWAII

By M.A. Scholl, S.E. Ingebritsen, C.J. Janik, and J.P. Kauahikaua

ABSTRACT

Isotope tracer methods were used to determine flow paths, recharge areas, and relative age for ground water in the Kilauea volcano area on the Island of Hawaii. Stable isotopes in rainfall show three distinct isotopic gradients with elevation, which are correlated with tradewind, rain shadow, and high-elevation climatological patterns. Temporal variations in isotopic composition of precipitation are controlled more by the frequency of large storms than by seasonal temperature fluctuations. Consistency in results between two separate areas with rainfall caused by tradewinds and thermally-driven upslope airflow suggests that isotopic gradients with elevation may be similar on other islands in the tradewind belt, especially the other Hawaiian Islands, which have similar climatology and temperature lapse rates.

Areal contrasts in ground-water stable isotopes and tritium indicate that the volcanic rift zones compartmentalize the regional ground-water system. Tritium levels in ground water within and downgradient of Kilauea's rift zones indicate relatively long residence times. Part of Kilauea's Southwest Rift Zone appears to act as a conduit for water from higher elevation, but there is no evidence for extensive down-rift flow in the lower East Rift Zone.

INTRODUCTION

Purpose and Scope

The near-surface rocks of many volcanic islands are highly permeable, and infiltration rates can be extraordinarily high. As a result, surface water is generally scarce and residents depend mainly on rain catchment systems and ground water for their water supply. In the southeastern part of the Island of Hawaii, perennial surface water is nearly absent despite an average rainfall of about 2,000 mm per year. The area studied covers 4,200 km^2 and encompasses all of Kilauea volcano and the surrounding slopes of Mauna Loa volcano (fig. 1). Wells in this part of Hawaii are concentrated north and west of the area enclosed by Kilauea's rift zones and are generally located within 10 km of the coastline (below ~300 m in elevation). As a result, ground-water flow patterns in and around Kilauea Volcano are not well-known.

The fact that isotopic content of rainfall can vary in a characteristic fashion with geographic location (due to differences in temperature, elevation, latitude, and distance from the coast) has been used in many hydrologic studies (Gat, 1971; Fontes, 1980; many others). Differences in isotopic content of precipitation with elevation are used to infer

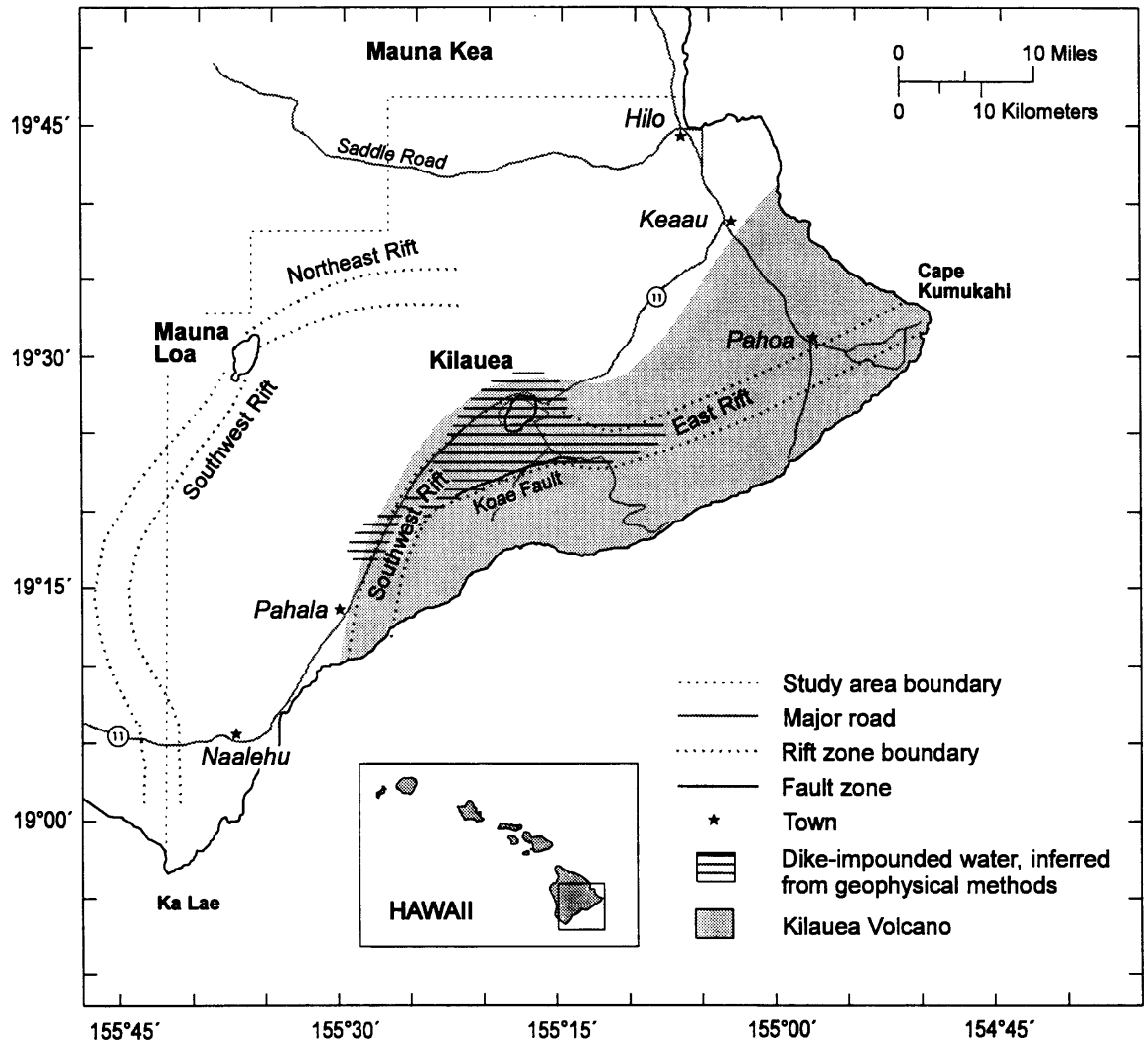

Figure 1. Map of the study area on the Island of Hawaii, showing geographic features discussed in the text.

recharge areas for ground water, to indicate mixing, or to delineate different ground-water systems. On Hawaii, mean temperatures range from 23.3°C at Hilo (sea level) to 7.0°C at Mauna Loa Observatory (3,400 m), so there is good potential for use of stable isotopes as tracers for ground-water flow. The purpose of this study was to use isotope techniques to interpret the regional hydrology of the Kilauea volcano area, and to determine precipitation isotope patterns in a general sense so that similar methods can be used in hydrologic studies on other islands, especially the other Hawaiian Islands. A network of as many as 66 precipitation collectors was emplaced in the study area and sampled at approximately six-month intervals from August 1991 to August 1994. The samples were analyzed for the stable isotopes of water, deuterium (D) and oxygen-18 (^{18}O). Ground-water wells, ground-water discharge along the coast (coastal springs and cracks), and high-elevation springs were sampled in

August/September 1991, '92 and '93. The ground-water samples were analyzed for chemistry, D, and ^{18}O, and a subset was analyzed for tritium (^{3}H).

Geologic Structure as Related to Hydrology

The rock in the study area is primarily tholeiitic basalt from Kilauea and Mauna Loa, with interspersed ash layers and some buried soils on the flanks of Mauna Loa. The layered structure of the basalt flows creates an anisotropic permeability structure, with horizontal permeability on the order of 10^{-9} to 10^{-10} m^2 (Ingebritsen and Scholl, 1993) and vertical permeability perhaps 10-1,000 times less (Souza and Voss, 1987). Volcanic rift zones are another source of heterogeneity. Mauna Loa and Kilauea, like other active basaltic volcanoes, are characterized by rift zones (fig. 1) radiating out from the summit area, along which magma travels to feed eruptions. The rift zones are repeatedly intruded by thin (less than 2 m), nearly vertical, subparallel dikes of dense basalt. Both Kilauea's East Rift Zone (ERZ) and Southwest Rift Zone (SWRZ) are thought to have migrated southward over time, and subsurface dikes are inferred to extend some distance north and west of the current surface expression of the rift zones (Swanson and others, 1976; Kauahikaua, 1993). The Koae fault zone south of Kilauea Crater is also thought to be a plane along which dikes are intruded, forming a barrier to ground-water flow and impounding water to high levels in the summit area (Jackson and Kauahikaua, 1990).

Occurrence of Ground Water

Previous workers (Stearns and Clark, 1930; Stearns and Macdonald, 1946; many others) have classified Hawaiian ground water in terms of three types or occurrences: basal, perched, or dike-confined. Basal ground water is areally extensive and occurs as a fresh-water lens floating on seawater that saturates the interior of the island. In a simplified conceptualization (hydrostatic conditions, sharp interface between fresh and salt water) the fresh water extends to a depth below sea water about 40 times the height of the water table above sea level. In reality, heterogeneities, flow and dispersion affect the thickness of the lens and create a transition zone at the interface, with mixing of the salt and fresh water. Basal ground water discharges at or below sea level at numerous places along the coast of the island, as suggested by simple water-balance calculations (Stearns and Macdonald, 1946) and evidenced by numerous springs and by infrared aerial photography (Fischer and others, 1966). Basal ground water can be sampled in wells, at springs along the coast at low tide, or where features such as cracks have exposed the water table. Near coastal discharge points, basal water is brackish to varying extent. In general, basal water flows from inland recharge areas where the water table may be several meters above sea level, to the shore, where the water table is near sea level.

Perched water is defined as water held above the basal lens by low permeability features such as ash layers, dense lava flows, soil, or alluvium, with an unsaturated zone between the perched water body and the basal lens. Perched

water bodies are generally not areally or vertically extensive. Perched water can be sampled at wells and springs.

In the volcanic rift zones, low-permeability dikes have intruded vertically across the horizontal high-permeability zones of lava flows. Dike intrusions in the rift zone can impound ground water to altitudes substantially above the level of the basal lens. The impounded water may flow parallel to the rift zone, leak out of the rift zone to the basal lens, and (or) be effectively compartmentalized by intersecting dikes. Rift zones may affect the rate and direction of flow of surrounding basal ground water, depending on the density of dikes in the rift zone and the orientation of the rift zone to regional ground-water flow. Dike-impounded reservoirs are an important water source on Oahu (Takasaki and Mink, 1985), and dike-impounded water probably exists in Mauna Loa and Kilauea's rift zones, but there is little direct evidence. Deep geothermal exploration wells drilled on the mid- to lower ERZ (East Rift Zone) of Kilauea volcano did encounter water levels above the surrounding basal lens, but water levels in shallow wells in the lower ERZ are not significantly higher than those outside the rift zone (Sorey and Colvard, 1994). Resistivity and self-potential measurements (Jackson and Kauahikaua, 1987, 1990; Kauahikaua, 1993) indicate that the high-level water (615 m) found in a deep drillhole beneath Kilauea summit (Keller and others, 1979) is part of an areally extensive water body that extends some distance down both Kilauea's ERZ and SWRZ (Southwest Rift Zone) (fig. 1).

Wells that tap the basal ground-water lens in the study area are generally located below 300 m elevation. However, recent drilling at elevations from 400-550 m has revealed vertically extensive ground-water saturation in three separate areas on Hawaii. Water levels were found to be about 300 m, higher than expected for a basal lens and in areas not known to contain dike intrusions (William Meyer, USGS, Honolulu, written commun., 1995). Therefore, ground water may not be at great depth below the surface in all higher elevation areas.

Climate and Rainfall

The climate of the Hawaiian Islands is dominated by tradewinds from the east-northeast, which blow more than 90 percent of the time in summer, and less frequently in winter. In winter, other weather systems (stationary highs, migratory highs, migratory low-pressure systems, and frontal systems) influence Hawaiian weather (Schroeder, 1993). A temperature inversion in the atmosphere at approximately 2,000 m elevation above sea level is a persistent feature of the tradewind pattern. The inversion is a boundary above which the tradewind clouds evaporate.

The interaction of the tradewinds with topography causes great areal variations in rainfall. Rainfall in the study area ranges from less than 500 to greater than 6,000 mm per year (fig. 2). The study area can be divided into 3 rainfall regimes; tradewind-dominated (south and west of Hilo and Pahala to Naalehu), rain-shadow (southwest of Kilauea summit), and high-elevation (above 2,400 m on Mauna Loa). South

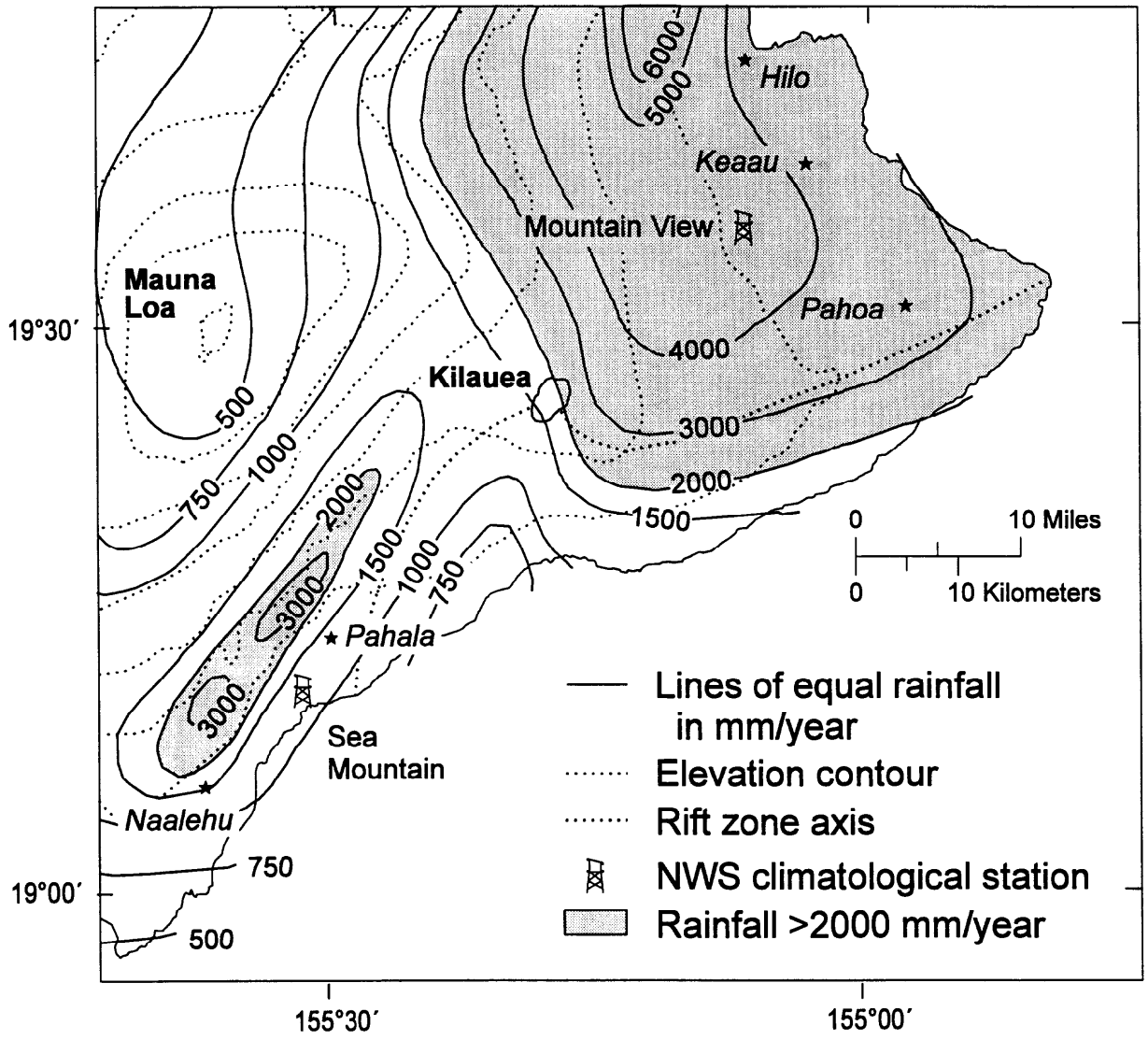

Figure 2. Median annual rainfall in the study area, in millimeters per year, from Giambelluca and others (1986). Elevation contour interval is 500 m.

and west of Hilo, the tradewinds move moist air masses up the flank of Mauna Loa. As the air cools, precipitation occurs, leading to near-daily rainfall and the highest annual rainfall in the study area. The area between Pahala and Naalehu is a southeast-facing slope; the frequent rainfall in this area is thought to be caused by a combination of tradewinds and a thermally-driven sea breeze/land breeze cycle (Giambelluca and Sanderson, 1993). Tradewinds flow downslope past the summit of Kilauea (1,225 m elevation), causing a rain shadow on its southwest flank. This area receives rainfall from storm systems unrelated to tradewinds, or when tradewinds are accentuated by a frontal system to the northeast of the Islands (T.A. Schroeder, Univ. Hawaii, written commun., 1995).

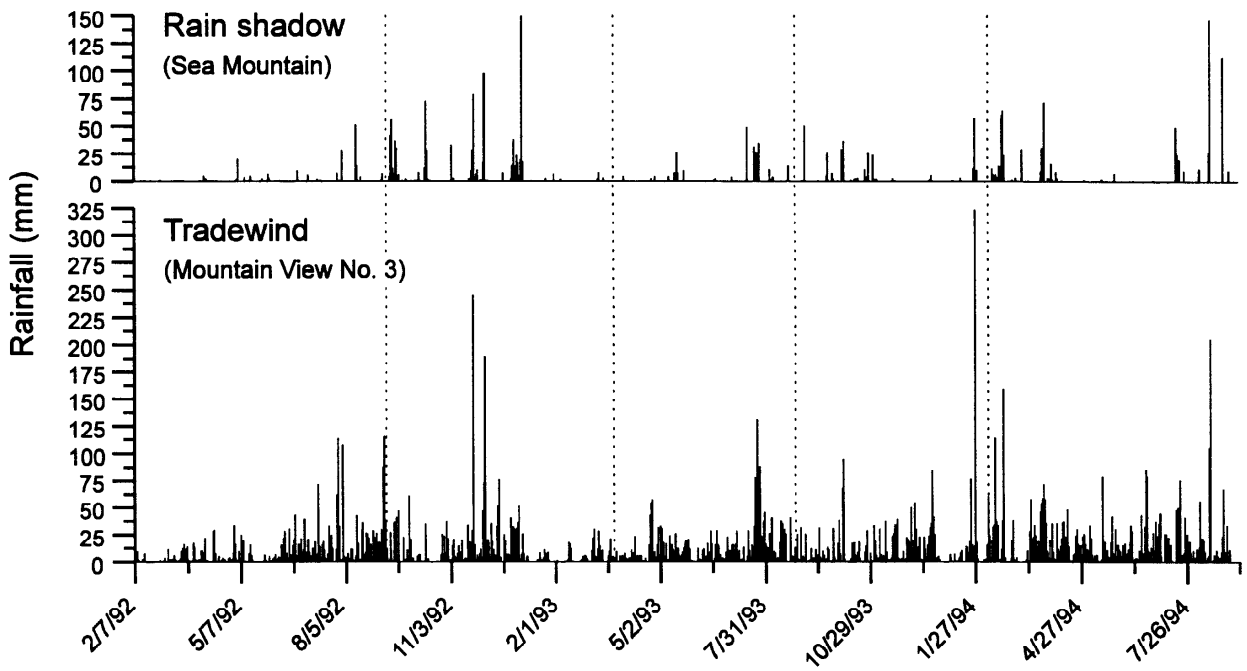

Figure 3. Daily rainfall in millimeters, 2/7/92 through 8/29/94, for Sea Mountain 12.15 station (index no. 51-8600-6) and Mountain View No. 3 station (index no. 51-6546-6) (Climatological Data, 1992-1994). Vertical dotted lines divide sample collection periods.

Winter frontal systems and 'Kona storms' from the south are a major source of rainfall to the leeward sides of all the Hawaiian islands (Blumenstock and Price, 1967, Schroeder, 1993). Kilauea summit itself has a sharp gradient in precipitation: the annual rainfall decreases by 1,250 mm per year over five kilometers from the northeast to the southwest side of Kilauea Crater (Giambelluca and Sanderson, 1993). The upper slopes and summit of Mauna Loa (4,145 m) are above the tradewind inversion. Rainfall above 2,400 m elevation is infrequent, occurring only during storms.

Rainfall records for two weather stations with different precipitation regimes are shown in figure 3. Mountain View station (fig. 2) is at 457 m elevation, midslope in the tradewind-affected area. There are very few dry periods; measurable rainfall occurs nearly every day. Sea Mountain station (fig. 2) is the station closest to Kilauea's rain shadow at which rainfall is measured daily. At this station, most rainfall occurs in discrete events.

Mechanisms for Differences in Rainfall Isotopic Composition

Dansgaard (1964) established that the condensation of precipitation from atmospheric vapor was analogous to an open-system Rayleigh-type distillation, described by:

$$\delta_c = \frac{\alpha}{\alpha_0} F_v^{\alpha_m - 1} - 1,$$

$$\delta_v = \frac{1}{\alpha_0} F_v^{\alpha_m - 1} - 1,$$

where δ_c and δ_v are the delta value (definition on p. 8) of condensate and vapor; α, α_0 and α_m are the isotopic fractionation factors at the condensation temperature, the initial temperature, and the mean temperature; and F_v is the remaining fraction of original vapor. Dansgaard noted that actual rainfall composition falls somewhere between the closed system analogy, where vapor and condensate remain in equilibrium, and the open system analogy, where condensate is continuously being removed from contact with the original vapor, and that in nature, exchange with other sources of vapor would alter the composition predicted by the Rayleigh equations. Later studies used a two-phase Rayleigh model to describe the rainfall process, with the cloud containing liquid water in equilibrium with vapor in addition to condensate leaving the system (Craig and Gordon, 1965, Gat and Dansgaard, 1972). The fact that the Rayleigh distillation model agreed fairly well with precipitation isotope data collected worldwide indicated that differences in rainfall isotopic content are controlled primarily by condensation temperature and the amount of moisture previously rained out of an air mass. Later studies showed the importance of exchange with local sources of atmospheric moisture, due to processes such as recycling of moisture due to evaporation from large water bodies and transpiration from plants, or mixing with atmospheric vapor from immediately above the ocean surface (Salati and others, 1979; Ingraham and Taylor, 1991; Yonge and others, 1989; Ingraham and Craig, 1993; Gat and others, 1994).

Previous Isotopic Studies

Few previous studies report water isotope values in the study area. Published precipitation isotope data are available only for Hilo and the upslope area in the saddle between Mauna Loa and Mauna Kea. Friedman and Woodcock (1957) measured deuterium in rainfall at four elevations up the Saddle Road (fig. 1) during a study of the tradewind-generated orographic rainfall. Deuterium values decreased with increasing elevation, but the small number of samples precluded any specific conclusion as to whether the 'rainout effect' or the 'temperature effect' was responsible for the decrease. McMurtry and others (1977) collected stable isotope data for twenty springs and wells in the Kilauea area as part of a survey of potential geothermal sites. They found all the ground-water samples in the area to be depleted in D and ^{18}O relative to Hilo precipitation, and concluded that most of the ground water had originated as recharge at elevations between 0 and 1,219 m. However, they did not measure rainfall to obtain the elevation gradient. Hsieh and others (1994) measured ^{18}O in rainfall on the leeward side of Kohala Peninsula, the northern tip of the Island of Hawaii, and found values ranging from -0.97 per mil to -13.7 per mil in monthly samples along a transect from 77 to 1,250 m in elevation.

Tritium measurements for the HGP-A well and some nearby water-supply wells in the lower ERZ area were published by Kroopnick and others (1978). Stable isotope and tritium measurements in rainfall were published for the International Atomic Energy Agency (IAEA) collection sites in Hilo and

on Midway, Wake and Johnston Islands from 1963 to 1984 (IAEA). Preliminary results from the first year of this study were published in Scholl and others, 1993.

Acknowledgments

We thank L. Douglas White and Mark Huebner for analyzing the stable isotope samples, and Robert Michel for analyzing the 1991 and 1994 tritium samples. Elizabeth Colvard, Frank Trusdell, Lynne Fahlquist, Kari Cooper, Cheryl Gansecki, Gary Puniwai, Gordon Tribble, and the Hawaii County Dept. of Water Supply assisted in sample collection. Special thanks are owed to Thomas Schroeder and Kevin Kodama of University of Hawaii Meteorology Dept. for insights into the climatology. We also acknowledge Kahuku Ranch, Mauna Loa Macadamia Nut, Inc., Alan Yoshinaga of Mauna Loa Observatory, Dennis Ida of Univ. Hawaii Agricultural Experiment Stations, Jack Minassian of Hawaii Volcanoes National Park, Tony and Koi Lee, Marilyn and Howard Haymore, Bobby Camara, Robert Koyanagi, and Patricia Shade for keeping rain collectors on their property. Paul Eyre, Stuart Rojstaczer, and Clifford Voss contributed substantially to the report with helpful reviews.

SAMPLE COLLECTION METHODS

Stable isotope values in this report are in δ-notation, which represents the ratio (R) of $^{18}O/^{16}O$ or $^{2}H/^{1}H$ in the sample to that of a standard (Vienna Standard Mean Ocean Water (VSMOW), Gonfiantini, 1978) in per mil (‰) units, so that $\delta = ((R_{sample} - R_{standard})/R_{standard}) \times 1000$. The standard error is 0.2 per mil for the $\delta^{18}O$ analysis and 2 per mil for the δD analysis.

Precipitation

Precipitation collectors were emplaced in the study area for the period August 1991 through August 1994. In 1991-93, a network of approximately 60 collectors was emplaced (fig. 4). In 1993-94, the network was reduced to 14 collectors. Collectors were designed to collect stable isotope samples; however, chemical analyses were also done on most of the samples to obtain information on the chemistry of recharge waters and deposition patterns of sulfate and chloride (Scholl and Ingebritsen, 1995). The precipitation collectors were sampled at 6-month intervals.

Precipitation collectors used in the study were 13- or 19-liter high-density polyethylene (HDPE) buckets with o-ring sealed lids, of the type used for liquid product packaging. Funnels of 5 cm, 8 cm, or 14 cm diameter were set in the lids, depending on the amount of rainfall expected at each site. At the end of the collection period, the volume of rainwater was measured either by weighing the collector, or (for sites accessible by foot only) by measuring the water level in the collector. Samples for isotopic analysis were passed through a coarse qualitative filter to remove oil and (or) particulate matter.

The collectors were designed to minimize sample evaporation. Three designs were used during the course of the study. For the first sample period

(8/91-2/92) collectors had 5-cm funnels and contained a 3-4 mm layer of silicone oil. This design proved flawed; weight loss from indoor controls and an isotopic shift in the field control showed that there was some evaporation through the layer of oil. The degree of isotopic shift in a 6-month sample depended on the total volume of sample and the temperature and humidity conditions around the collector. The isotopic shift that occurred in the controls was enrichment *along the meteoric water line*, so that the evaporation would have been undetected in the absence of controls. Different collector designs were used for subsequent sample periods, although at some sites where animal damage or accessibility was a problem, oil-type collectors were still used, with an 8 mm layer of oil. Controls showed that 0.6 per mil or less enrichment in ^{18}O occurred with the 8 mm layer of oil.

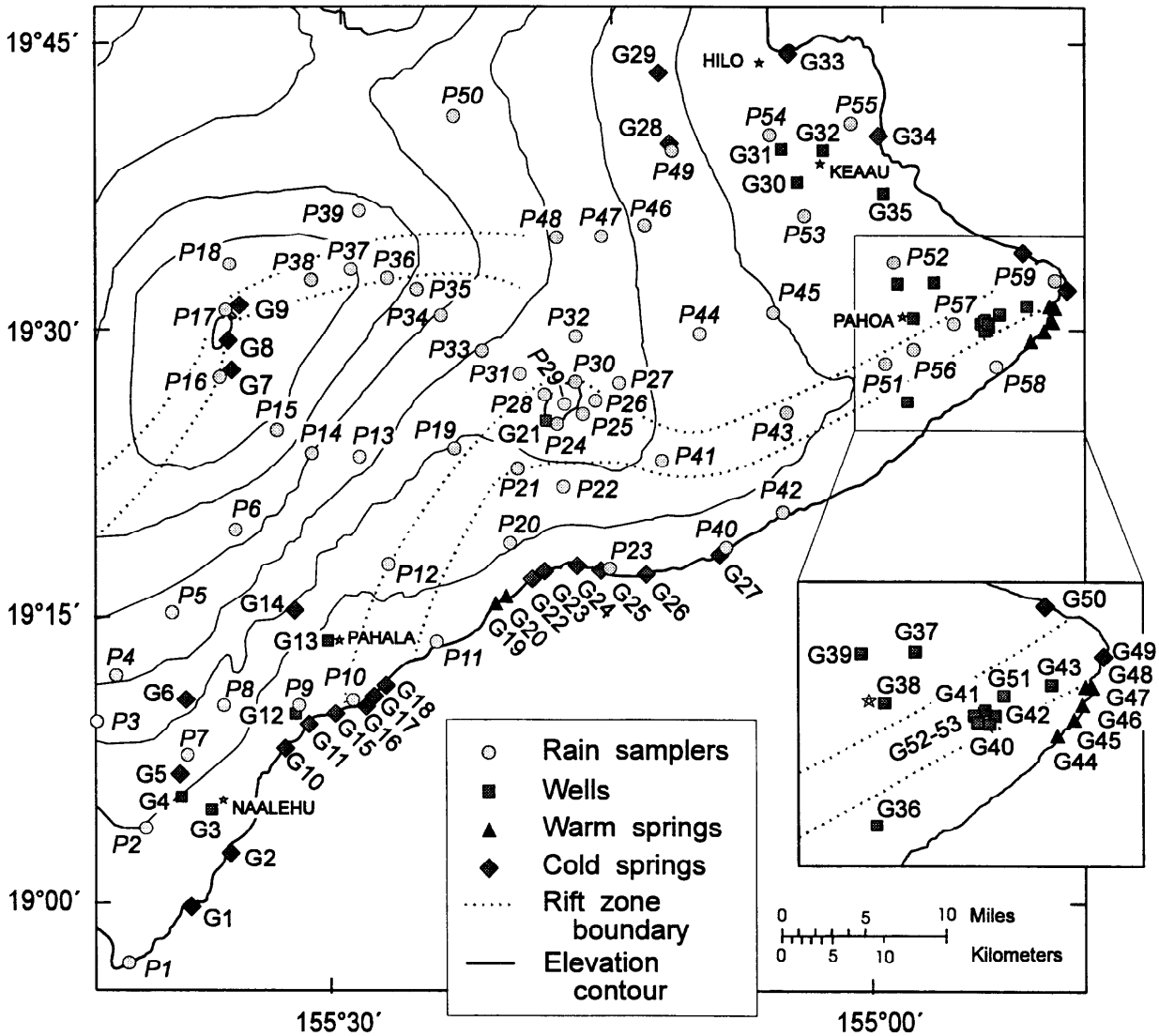

Figure 4. Locations of precipitation sample sites (P1-P59) and ground water sample sites (G1-G52). Elevation contour interval is 500 m.

Two modified collector designs were used for subsequent sampling periods. At open-sky sites, the funnel contained a plastic ball that floated when the funnel was full and covered the opening at other times (M.L. Davisson, Univ. California Davis, oral commun., 1991). Orchard netting was placed over the funnel to keep out large debris. At forested sites, the bucket contained a polypropylene bag and the funnel contained polyester fiber to filter debris. A piece of plastic tubing attached to the funnel stem extended to the bottom of the bag, and both bag and bucket had 1 mm air outlet holes. The bag filled gradually, leaving little airspace to be occupied by vapor. For both these designs, evaporation measured by weight loss in controls did not exceed 0.04 g/day, and isotopic shift in field controls was undetectable.

All the collector designs had certain drawbacks. The ball-in-funnel collectors were occasionally found with leaves or dead insects interfering with the ball function. The bag collectors tended to grow algae in the sample, sometimes to the point of blocking the inlet tubing. The bag collectors also had smaller capacity than the bucket volume, so that they overfilled at a few sites. If the collector was found damaged at the end of the six-month collection period, the sample was not analyzed for isotopes. This report does contain some data from overfilled collectors, in cases where that is the only measurement available for the site (as noted in Appendix 1).

At sites where we had a collector within 15 m of a standard rain gage, collector efficiency was estimated by comparing rainfall collected in our samplers to rainfall measured in the standard gage over the same time period (Climatological Data, 1992-1994). Apparent collector efficiency for our samplers ranged from 54 percent to 116 percent; most were within 85 - 110 percent. The poorest agreement between a standard gage and our collector was at a site where the collector was near a building. Precipitation in the study area was up to 50 percent below normal during the first year of the study, but near normal for the subsequent periods.

Ground Water

Ground-water samples (fig. 4) were obtained from four sources: 1) wells; 2) ground-water discharge at or just below sea level (coastal springs); 3) cracks or pools in the basalt near the shoreline, where the basal lens is exposed (cracks); and 4) discharge at elevations above 300 m (high-level springs or streams). Most of the wells sampled were water-supply wells with pumps installed. These extend no more than 46 m below sea level (penetrating 5 to 45 percent of the estimated freshwater lens thickness), and are generally uncased or have perforated casing for the entire saturated interval. If the well was not being pumped at the time of sampling, it was pumped for 15 minutes before sampling. Wells with no pump were sampled from the top of the water column. The coastal springs and cracks were sampled at low tide, when possible. Samples were generally collected within 45 cm of the surface of the water in cracks or pools.

Most ground-water sites were sampled three times, in August or September of 1991, 1992, and 1993. Samples were analyzed for $\delta^{18}O$, δD and

chemistry; a subset was analyzed for ^{3}H (tritium). Temperature and pH were measured at time of sampling. (see Janik and others, 1994, for chemical analyses of the 1991 and 1992 samples).

The coastal springs and cracks are brackish, and samples contained varying amounts of seawater. Assuming that the samples were a mixture of seawater and fresh meteoric water, the chloride concentration was used to correct for seawater content and obtain the isotopic composition of the freshwater end-member, using seawater Cl at 18,900 mg/L, ground-water Cl at 5 mg/L, and seawater at $\delta^{18}O$ and δD of 0 per mil (SMOW). The calculated seawater content for the samples ranged from less than 1 percent to 60 percent. Stable isotope results for ground water and seawater are shown in Appendix 2.

INTERPRETATION OF STABLE ISOTOPE AND TRITIUM DATA

Stable Isotope Composition of Rainfall

Data from the rainfall isotope collections are listed in Appendix 1. Because isotopic composition of rainfall varies seasonally, volume-weighted averages were calculated on the basis of summer-winter pairs to obtain a yearly average. For some sites, there is only one summer-winter pair, for others, two summer values and one winter value, and so forth. Thus the final average isotopic value is better for some sites than others. The volume-weighted average for each site was calculated in two steps; first the volume-weighted average was found for each summer-winter pair, then the volume-weighted average of all summer-winter averages was taken as final. Data from the first collection period are not reported here or used in the calculation of the average, because the samples evaporated to a variable and unknown degree.

Figure 5 shows δD relative to $\delta^{18}O$ for rainfall from five 6-month collection periods, plotted with the global meteoric water line (Craig, 1961) for comparison. Previous data from the IAEA network show that rainfall stable isotopes for many tropical islands plot above the global meteoric water line, on a trend with a slope of about 6, because of the proximity to a source of water vapor in isotopic equilibrium with ocean water (Dansgaard, 1964; Yurtsever and Gat, 1981). Some low-elevation rain samples from spring-summer 1993 do fall along a trend with a slope lower than 8 (fig. 5C), but the volume-weighted average samples for the entire study period define a local meteoric water line ($\delta D = 8.0\ \delta^{18}O + 12$) having the same slope as the global line.

Seasonal Variations in Stable Isotopes in Precipitation

Data from the worldwide IAEA network have also shown isotopic composition of rainfall in most areas to follow a seasonal cycle, with more depleted isotopic composition in winter and more enriched composition in summer, due to seasonal temperature variation. There are exceptions to this rule, and the IAEA station at Hilo is one of them (Yurtsever and Gat, 1981). The data in this study do show a seasonal cycle for 1992 and 1993 (fig. 6), despite a relatively small seasonal variation in

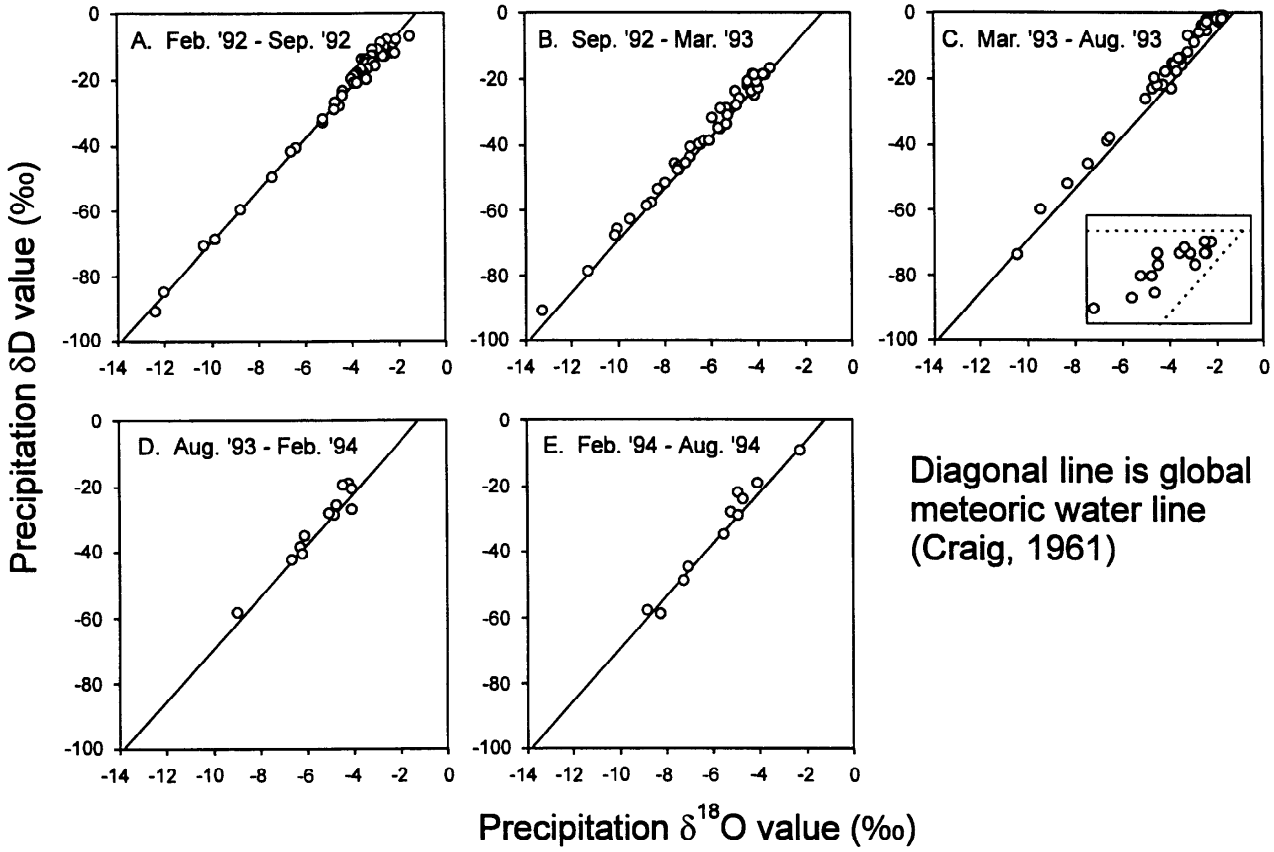

Figure 5. Stable isotope ratios in six-month cumulative precipitation samples from the southeast part of the Island of Hawaii.

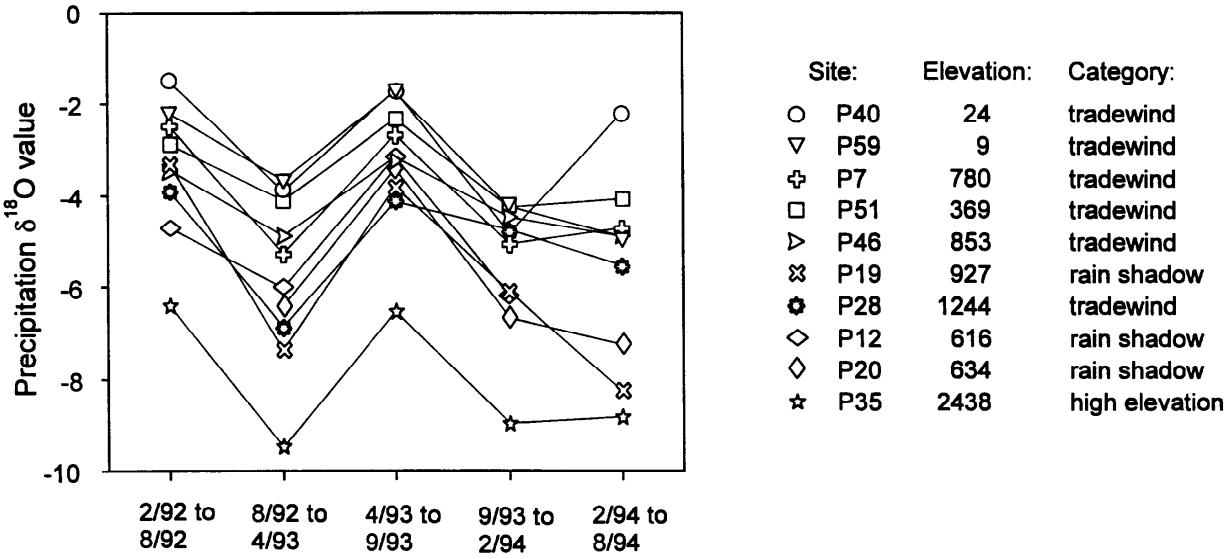

Figure 6. Variation in $\delta^{18}O$ values for precipitation at 10 sites where a sample was collected each sampling period.

temperature (ranging from 2.8°C in Hilo to 3.8°C at Mauna Loa Observatory). However, no seasonal cycle is evident in the 1994 data, except at site P40 (fig. 6). Some samples from the 1994 spring-summer period were even more isotopically depleted than the preceding fall-winter values.

Reasons for both the seasonal cycles in isotopic composition and the extremely depleted spring-summer values in 1994 can be inferred from the rainfall record (fig. 3). During the 1992-93 collection periods, the number of storms was higher during the winter months at both the tradewind and rain shadow stations. (Storms are defined here as one or more consecutive days of rainfall greater than 50 mm). During the summer of 1994 there were more storms than in the previous summer periods. Tradewind rains are generated no higher than the inversion, at 1,800-2,400 m elevation, where the minimum temperature is about 11°C. Storms extend much higher into the atmosphere, with condensation at 4,000 to (possibly) 6,000 m (T. A. Schroeder, Univ. Hawaii, written commun., 1995). Condensation temperatures are cooler at these higher altitudes, leading to a larger degree of fractionation for the water isotopes. Also, in contrast to the tradewind-generated orographic rainfall, which is the first condensation from moist air above the ocean, large storm systems may have been raining for some time before they reach the island. The lower temperatures, combined with the likelihood that storm systems are raining before they reach land, would lead to much more depleted isotopic composition for storm precipitation. We collected one isotope sample directly from a tropical storm, and it supports this inference. That sample was taken at the coast (site G45 on fig. 4), and had isotopic composition of $\delta^{18}O$ = -5, δD = -32; the longer-term volume-weighted average for that area is -3.2, -15 (site P58 on fig. 4).

We hypothesize that the proportion of storm versus tradewind or thermally-driven orographic precipitation controls seasonal variations in the isotopic composition of precipitation in the study area. Higher frequency of storms is usually, but not always, correlated with the winter months. In northern Taiwan, an opposite seasonal pattern occurs; winter rains have more enriched isotopic composition than summer rains, corresponding to the change from a northeast to a southwest monsoon (Liu, 1984). Friedman and others (1992) also found that almost all seasonal differences in isotopic content could be explained by differences in winter-summer storm trajectories for Southern California. We recognize that seasonal temperature differences must also influence precipitation isotopes on Hawaii, as there are seasonal differences in areas that receive only storm rainfall. The seasonal fluctuations are greatest for sites with a larger proportion of storm rainfall, in the rain-shadow and high-elevation areas (fig. 6).

Throughfall

The higher-rainfall parts of the study area are densely vegetated. In the period from February to August 1992, duplicate collectors were placed at several sites, with one collector in a location open to the sky and one collector under trees or

vegetation. We obtained samples from five open-sky/throughfall pairs (table 1).

Table 1. Comparison of volume and isotopic content of precipitation, for sites where open-sky (OS) and throughfall (TF) duplicates were placed. See Appendix 1 for further information about these sites.

Site	Type	Elevation, (m)	Volume, (L)	$\delta^{18}O$	δD
P19A	OS	927	9.20	-3.3	-17
P19B	TF		1.19	-4.4	-25
P25A	OS	1134	1.47	-3.8	-18
P25B	TF		1.43	-3.9	-19
P33B	OS	1524	7.24	-2.1	-12
P33C	TF		1.11	-4.5	-28
P42A	OS	23	1.33	-2.3	-12
P42B	TF		0.67	-2.6	-13
P46A	OS	853	2.99	-3.4	-15
P46B	TF		5.34	-3.5	-14

Kendall (1992) found throughfall samples in a Georgia watershed to be isotopically enriched relative to open-sky rainfall. In contrast, the throughfall samples in this study either had similar or more depleted isotopic composition than open-sky duplicates. The two throughfall collectors that had more depleted isotopic composition than their open-sky counterparts may have received predominantly storm rain, with the vegetative cover tending to block out drizzle and light rainfall from tradewind processes. It also appears that vegetative canopy can either block rainfall (sites P19, P33, P42) or enhance amounts of rain or fog drip collected in throughfall containers (site P46).

Relation Between Rainfall Stable Isotope Composition and Elevation

Volume-weighted average rainfall $\delta^{18}O$ values were plotted against elevation of the sample site, and regression lines were determined for the tradewind, rain shadow, and high-elevation areas (fig. 7). High-level spring, stream, and Hilo IAEA data were included with the volume-weighted average rainfall data for the regressions; Mauna Loa summit crack data were not used. The relation between precipitation isotope values and elevation (in meters) defines three distinct linear trends:

(1) Tradewind areas:

$\delta^{18}O = -0.00164$ (elevation) - 2.85, $r^2 = .90$
$\delta D = -0.0123$ (elevation) - 11.2, $r^2 = .80$

(2) Kilauea's rain shadow:

$\delta^{18}O = -0.00148$ (elevation) - 4.44, $r^2 = .80$
$\delta D = -0.00978$ (elevation) - 26.7, $r^2 = .75$

(3) High-elevation area:

$\delta^{18}O = -0.00319$ (elevation) - 0.45, $r^2 = .97$
$\delta D = -0.0259$ (elevation) + 9.3, $r^2 = .96$

In the 'east-side' tradewind and 'west-side' tradewind/thermal circulation rainfall areas (fig. 7), the $\delta^{18}O$-elevation relation is the same. In Kilauea's rain shadow, isotopic values fall along a trend that has a similar slope to the trend for the tradewind areas, but has an intercept that is about 1.6 per mil more depleted in $\delta^{18}O$. The high-elevation data follow an elevation trend with a distinctly different slope than either the tradewind or rain shadow data.

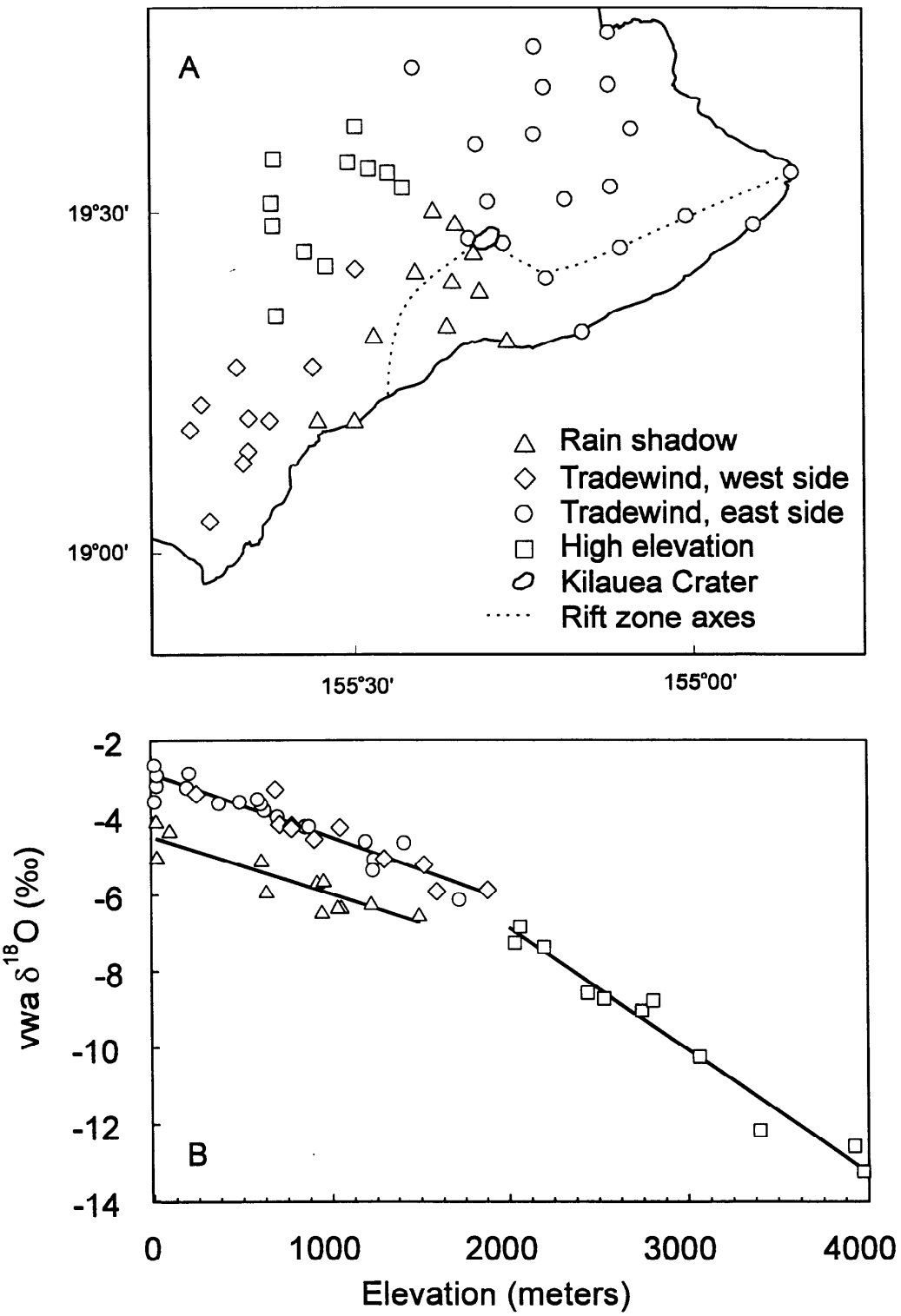

Figure 7. A) Map of study area, showing sites used in the regressions in the text, which are illustrated in 7B. Symbols denote areas with different climatology, as defined by isotopic relation with elevation in 7B. B) Relation between volume-weighted average $\delta^{18}O$ values and elevation in the study area.

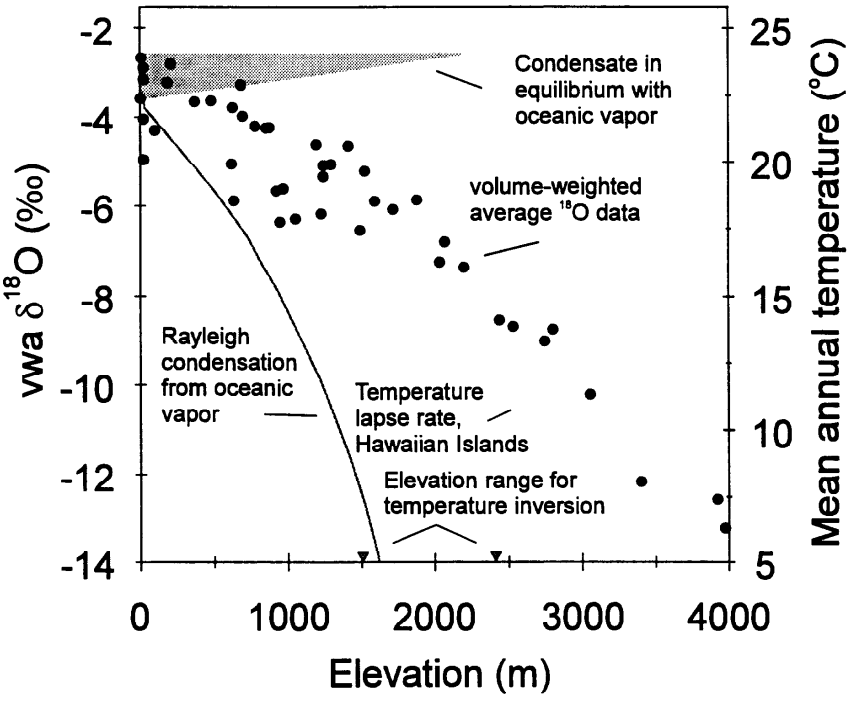

Figure 8. Comparison of data from figure 7B with calculated $\delta^{18}O$ values for condensation, range of $\delta^{18}O$ values for condensate in equilibrium with oceanic vapor at temperatures between the land surface and the inversion layer, and average temperature lapse rate for the Hawaiian Islands.

Figure 8 shows the same volume-weighted average $\delta^{18}O$ data plotted against elevation, along with the approximate temperature lapse rate for all the Hawaiian Islands (Nullet and Sanderson, 1993) and a Rayleigh condensation curve. The curve shows the change in condensate $\delta^{18}O$ composition for a parcel of oceanic vapor ($\delta^{18}O$ = -13 per mil: Craig and Gordon, 1965) that starts condensing at the shoreline and finishes at the average elevation of the inversion (about 2,000 m), without input of additional vapor from any source. The shaded triangular area shows the expected $\delta^{18}O$ content of condensate in equilibrium with oceanic vapor at the mean temperatures between land surface and the approximate top of the inversion layer (0 to 2,400 m). The relation between precipitation isotopes and elevation defined by most of the low-elevation data can be explained by mixing between depleted vapor from which some condensation has occurred and 'fresh' oceanic vapor, or by mixing of depleted vapor with vapor returned to the atmosphere by evapotranspiration, or both.

The tradewind rainfall data from the lowest elevations fall in the shaded range on figure 8, indicating that orographic lifting and condensation of water vapor from over the ocean is the predominant mechanism of rainfall in both tradewind areas. The land-surface slope is different in the two tradewind areas and, as noted previously, the 'west-side' (Pahala-Naalehu area) rainfall is attributed to a thermally-driven seabreeze cycle as well as tradewinds. The similarity of rainfall isotopic composition between the geographically and topographically distinct 'east side' (Hilo-Pahoa) and 'west side' (Pahala-Naalehu) areas suggests that the same isotope/elevation relation may apply to climatologically similar areas on other Hawaiian Islands, where the starting composition of the water vapor and the temperature

gradient with elevation would presumably be the same.

The more depleted isotopic content of rainfall in the rain shadow of Kilauea volcano likely is due to the fact that the area receives only storm rainfall, as previously discussed. It may be more difficult to explain why there is any gradient of isotopic content with elevation in the rain shadow at all, because in many continental areas leeward of mountain ranges, there is little suggestion of an isotopic gradient (for example Smith and others, 1979; Ingebritsen and others, 1994; Adams and others, 1995). In windward areas on Hawaii, there is a consistent orographic lifting effect, with upslope wind flow accompanying rainfall. Perhaps most of the storms that bring rain to Kilauea's rain shadow come from a southerly direction, generating upslope winds on the south side of the island.

We attempted to evaluate this possibility using climatological data. Rainfall records for the Sea Mountain station (fig. 3) were used to represent the rain shadow area. This station had measurable precipitation (at least 0.01 inch) on 320 of the 935 days of the study. Mountain View No. 3 station (fig. 3) represents the tradewind rainfall area. This station had measurable precipitation on 808 of the 935 days of the study. Wind speed and direction data (readings every 30 minutes) were obtained from two Hawaiian Volcano Observatory weather stations near Kilauea summit, one at the Observatory (2/92 to 2/93) and one at a site east of Kilauea Crater (2/93 to 9/94). Daily rainfall greater than or equal to 13 mm (0.5 inch) at the rain shadow station was assumed to be due to a storm system of some kind. Some of these rain events were large storms that affected the entire island; the dates include the 6 largest, and 10 of the top 15 largest daily rainfall measurements for the tradewind station. Rain events of 13 mm or more constituted 79 percent of the total rainfall for the rain shadow station, while those days accounted for only 22 percent of the total rainfall at the tradewind station.

The resultant daily wind speed and direction were calculated for each day that rainfall was 13 mm or more at the rain shadow station, using measurements greater than 1.75 miles per hour (the detection limit of the instrument). Only 20 of 49 large rain events at the rain shadow station were associated with south winds (resultant direction for the day = 90° to 270°) near Kilauea summit. However, for 11 of the 29 rain events apparently associated with north winds, rainfall was higher at the rain shadow (southern) station than at the tradewind (northern) station. One possible explanation is that some storms which came from the south had light or variable winds, so that the resultant wind direction was dominated by tradewinds that became re-established as the storm dissipated. In addition, wind measurements near Kilauea summit may not be representative of conditions in the rain shadow. Enough of the rain events in the rain shadow area (41 percent to 63 percent) were associated with storms that came onto land from a southerly direction to suggest that there may be an orographic rainfall effect during storms sufficient to cause an isotopic gradient with elevation.

At high elevations on the summit of Mauna Loa, the rate of decrease in δ-value with elevation is greater than in

the lower-elevation areas (figs. 7,8). Since there were fewer 6-month sample sites at high elevations, and rainfall is not measured daily at the local weather stations, it is difficult to correlate these isotopic results with weather patterns. We assume that the only source of precipitation is storms, because the area is above the tradewind inversion. Smith and others (1979) pointed out that isotopic fractionation factors change when condensation temperatures decrease to the point where condensation to a solid occurs. A theoretical model for a rising air mass (their fig. 2) shows that the rate of change of condensate δ-values with elevation should increase at elevations above about 3,000 m, where condensation occurs as snow rather than rain. Our data for the Kilauea area (fig. 7B) agree with this model. Both condensation of snow from a rising air mass and equilibration of solid condensate with temperatures at the collection site can explain our high elevation data, and without detailed information about the condensation processes in storms that affect the summit of Mauna Loa, both processes seem plausible.

At earlier stages of this study, before many precipitation data were obtained for the rain shadow area, the relatively depleted isotopic composition of ground water south of Kilauea summit was interpreted as indicating that springs at the coast were recharged at elevations above the summit (Scholl and others, 1992). As the study progressed, it became obvious that precipitation in the rain shadow area was substantially more depleted than in surrounding areas at similar elevation, such that the local precipitation within the rift zones could account for the ground-water isotopic composition. The spatial variation in precipitation isotopes observed in the study area suggests that in regions with highly variable microclimates and rainfall conditions, a detailed precipitation sampling network is necessary to avoid such misinterpretations.

Stable Isotope Composition of Ground Water

Ground-water sample locations, average chloride, and stable isotope composition (uncorrected and corrected for seawater content) are listed in Appendix 2. The stable isotope composition of water sampled at most sites varied little from year to year, as expected if sampling an extensive ground-water system. The largest variation (as indicated by the standard deviation) between yearly samples was seen in samples from water-filled cracks near the summit of Mauna Loa. The samples from the cracks appear somewhat enriched in heavier isotopes when compared with rainfall samples. The water in the cracks is often frozen, and the freeze-thaw cycle, combined with evaporation into the very dry air at that altitude, may cause isotopic enrichment. Large variations are also seen in the thermal (≥30°C) springs, where the seawater correction was large, and in some of the municipal wells, possibly due to differences in the pumping history prior to sampling.

Figure 9 shows average ground-water stable isotope ratios, unadjusted for seawater content, for sites sampled in 1991-93. The samples are generally

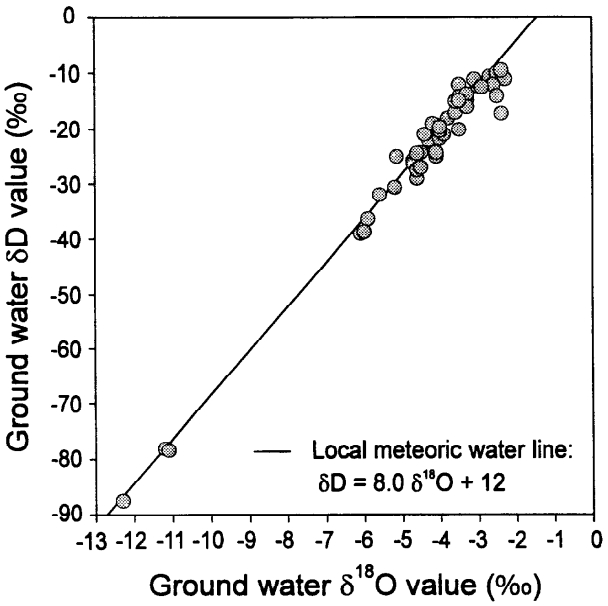

Figure 9. Stable isotope ratios for ground water. Data points are the average of samples taken 1991-93, unadjusted for seawater content.

within the range of -10 to -40 per mil for δD and -2 to -6 per mil for $\delta^{18}O$, except for the three samples from Mauna Loa summit. Samples to the right of the meteoric water line are affected by mixing with seawater. The largest departure represents samples from the brackish thermal spring at Puu Elemakule (Appendix 2; G19), which may have an ^{18}O shift due to reaction with rock at higher temperatures (Janik and others, 1994). For the other thermal waters sampled in the study, there is little or no evidence of ^{18}O shift.

Estimation of Recharge Elevations

The $\delta^{18}O$ composition of precipitation was used to estimate the source area of recharge to springs and wells. Interpretation of the recharge areas for ground water also included consideration of local geologic structure, recharge patterns, and sample type. For the pumped water-supply wells, the samples we collected may have been: 1) a mixture of the part of the freshwater lens penetrated by the perforated section of the well and within the area of influence of the pumping well, or 2) a sample biased toward a highly permeable layer of the aquifer. At the coastal cracks, the top of the water table was sampled, and at coastal springs, the accessible discharge was sampled, usually in the intertidal zone. At coastal locations, the samples may have represented: 1) local recharge contributing to the top of the freshwater lens, 2) a mixture of flowpaths from increasing distances upslope converging to a discharge point at the coast, or 3) discrete flow from one area upslope. In addition, in areas near the rift zones, samples may represent mixtures of dike-impounded water with local recharge.

Salinity and temperature profiles were measured in two 3.5 to 4 m deep cracks (G27 and G15 on fig. 4) using a conductivity/temperature probe lowered slowly down the crack. Salinity ranged from 11 percent to 15 percent of seawater in G27 and 3.5 to 4 percent of seawater in G15. Isotope samples taken from the top and bottom of each profile were not significantly different: At G27, $\delta^{18}O$ = -4.4, δD = -25 at the top and -4.4, -23 at the bottom; at G15 the values were -5.4, -29 at the top and -5.6, -31 at the bottom. The measurements indicated that sampling from just below the water surface in the coastal cracks was effectively the same as obtaining a sample from 3-4 m depth.

Recharge elevations for each spring and well were estimated in two ways. First, the linear fits to the data in figure

7 were used to calculate recharge elevations at which the measured isotopic content of the ground water matches the isotopic content of precipitation. The tacit assumption in this case is that the sample represents a single flowpath from one elevation. Second, we assumed that the isotopic content of the ground-water samples represents an integrated sample of recharge between the sampling point and some point upslope. This assumption might not be reasonable for confined ground-water systems, but seems plausible for the Kilauea area, where low-permeability layers that restrict recharge or separate aquifers are not likely to be areally extensive. The expected isotopic composition of water at the sampling point was estimated as:

$$\delta^{18}O_{sample} = \frac{\sum_{elev=1}^{n} (\delta^{18}O)_n \, (R)_n}{\sum_{elev=1}^{n} (R)_n}$$

where $(\delta^{18}O)_n$ is the isotopic value of precipitation for elevation interval n, obtained from linear regressions on the data of figure 7, and $(R)_n$ is the estimated recharge amount for the elevation interval n. Elevation intervals were 152 to 305 m. Recharge elevations were also calculated using δD for warm springs, in case there had been ^{18}O exchange with rock at some point in the history of the thermal water (table 2).

Recharge $(R)_n$ was estimated as rainfall minus pan evaporation (data in Ekern and Chang, 1985) in areas with rainfall greater than 1,500 mm per year, as 23 percent of rainfall for rates of 1,300-1,500 mm per year, 22 percent for 1,040-1,300 mm per year, 19 percent for 790-1,040 mm per year, and 13 percent for 530-790 mm per year. The recharge percentages for drier areas were based on estimates made for dry areas on Oahu (Eyre and others, 1986; Takasaki, 1993), but were arbitrarily increased by 5 percent for this study area, as there is less soil developed on Kilauea and Mauna Loa than on Oahu. The dry-area recharge estimates are very approximate. However, the calculated recharge elevations depend more on the relative contribution of water from each area upslope than on exact amounts, and are fairly insensitive to changes in the dry area recharge percentages. Another consideration is that the bulk rainfall samples may be more enriched than the water that actually recharges the ground-water system. Particularly on the south-facing slopes of the study area, it is possible that a disproportionate amount of storm rainfall (intense rainfall, isotopically depleted) recharges the ground-water system, whereas a disproportionate amount of tradewind-type rainfall (drizzle or light rain, isotopically enriched) is transpired or evaporated. As a result, the calculated recharge elevations (table 2) may tend to represent maximum possible flow path lengths.

The recharge elevation estimates for each spring or well are shown graphically on figure 11. The general conception for ground-water flow through most of the study area is that the water table is a subdued replica of the topography. This concept is supported by sparse water level data in the Kilauea area (Takasaki, 1993). For each sample site, therefore, the flowpath is drawn to extend directly upslope from the sampling point, perpendicular to topography, unless geologic and isotopic evidence suggest otherwise.

Table 2. Results of ground water recharge elevation estimates (in meters), showing average isotopic composition of ground water samples, elevation at which the composition of precipitation matches that of the ground water, and maximum elevation of a flow path along which the integrated composition of recharge matches the ground water sample. For high-elevation springs, selected wells, and streams only the matching elevation is shown. Samples with isotopic composition more enriched than local rainfall (---) have no recharge elevation estimates. For springs and wells >30°C, both $\delta^{18}O$ and δD were used to calculate recharge elevations. Samples 14, 11, 12, 8, 27, 26, 3, 9, 10 and 2 are from McMurtry et al. (1977). Samples WR and PSM are from Tilling and Jones (1995).

ID	State well number	Location	Avg. $\delta^{18}O$	Elev. match $\delta^{18}O$	Elev. integrated $\delta^{18}O$	Avg. δD	Elev. match δD	Elev. integrated δD
G1		Kaalualu springs	-5.0	1243	305 or >2743			
G2		Waikapuna spring	-4.9	1229	305 or >2743			
G3	0335-01	Naalehu well	-4.2	767	610			
G4	0437-01	Waiohinu exploratory well	-5.1	1263	>2743			
14		Honuapo Mill well	-3.9	639	609-762			
G5	0537-01	Haao spring[†]	-4.2	830				
G6	0936-01	Mountain House spring[†]	-4.3	914				
G10		Kawa spring	-4.2	830	1219			
G11		Punalu'u beach spring	-4.8	1219	>2743			
G12	0831-03	Ninole B (Sea Mtn.) well	-4.5	1005	152 or 2438			
11		Palima well	-6.7	1524	>1524			
G13	1229-01	Pahala well	-4.7	1128	>2743			
12		Pahala Mill Shaft	-5.4	1559[§]	>2743[§]			
G14	1331-01	Alili spring[†]	-4.6	1066				
G15		Crack near Kamehame Hill	-5.4	642[§]	1219[§]			
G16		Waioala spring	-6.2	1172	>1524			
G17		Pueo spring	-6.3	1239	>1524			
G18		Waiapele crack	-6.1	1113	>1524			
G19		Puu Elemakule spring	-4.7	186	305	-34	762	1219
G20		Opihinehe spring	-5.5	710	1142	-34	762	1219
G21	2317-01	Kilauea summit borehole	-5.6	762		-32	609	
WR		Wright Road wells[†]	-4.6	1066				
G22		Kaaha cracks	-5.1	457	762	-32	609	914
G23		Kalue crack	-5.1	457	762	-30	339	685
G24		Halape springs	-4.8	252	460	-28	152	304
G25		Keauhou beach spring	-4.9	317	609	-30	339	685
G26		Apua Point crack	-4.4		837	-24		805*

ID	State well number	Location	Avg. $\delta^{18}O$	Elev. match $\delta^{18}O$	Elev. integrated $\delta^{18}O$	Avg. δD	Elev. match δD	Elev. integ-rated δD
G27		Crack near Kaena Point	-4.4		837	-24		805*
8	2102-01	Pulama well	-4.0	700	1066	-21		
G28		Waiakea stream at gauge†	-3.5	395				
G29	4211-01	Olaa Flume spring†	-3.6	457				
G30	3603-01	Olaa well #3	-3.6	457	762			
G31	3804-01	Keaau (Shipman) well	-4.4	950	>2743			
G32	3802-03	Olaa #1 (Keaau Mill 1)	-4.2	822	2133			
27		Olaa mill well	-3.9	639	1219			
PSM		Puna Sugar Mill, Olaa	-3.8	577	1067			
G33		Waiakea Pond	-3.7	524	1067			
26		Hilo Electric well	-3.3	272	457			
G34		Haena beach spring	-4.1	761	2133			
G35	3588-01	Paradise Park well	-3.5	401	609			
G36	2487-01	Keauohana well	-3.3	304	450			
G37	3185-01	Hawaiian Beaches well	-3.3	304	380			
G38	2986-01	Pahoa 2A well	-3.6	457	703			
3		Kapoho landing strip well	-3.1	152	152	-14	152	304
G39	3188-01	Keonepoko Nui well	-4.0	700	>1524			
9		Allison well	-3.3	304	391	-17	457	686
10		Malama-Ki well	-1.6	---	---	-9	---	---
G40	2983-01	PGV MW-1 well	-3.0	50	3	-12	3	
G41	2883-07	PGV MW-2 well	-2.8	---	---	-11	---	---
G42	2983-02	PGV MW-3 well	-3.1	152	---	-11	---	
G43	3080-01	Kapoho Crater well	-3.4	342	457			
G44		Pohoiki spring	-3.1	152	152	-13	96	152
2		Allison spring	-2.2	---	---	-12	---	---
G45		Campbell spring	-2.8	---	---	-13	96	152
G46		Pualaa Park spring	-3.3	280	393	-13	96	152
G47		Kapoho Beachlots pond	-3.1	152	152	-14	152	304
G48		Vacationland pond	-2.8	---	---	-16	347	610
G49		Lighthouse spring	-3.3	304	393	-14	152	304
G50		Orr's spring	-3.7	518	914			
G51	2982-01	GTW-3 well	-2.6	---	---	-10	---	---

* elevation calculated assuming half tradewind rainfall source, half storm source.

†well with perched water or high-level spring or stream.

§median recharge elevation; ground water assumed to be a mixture of two separate sources.

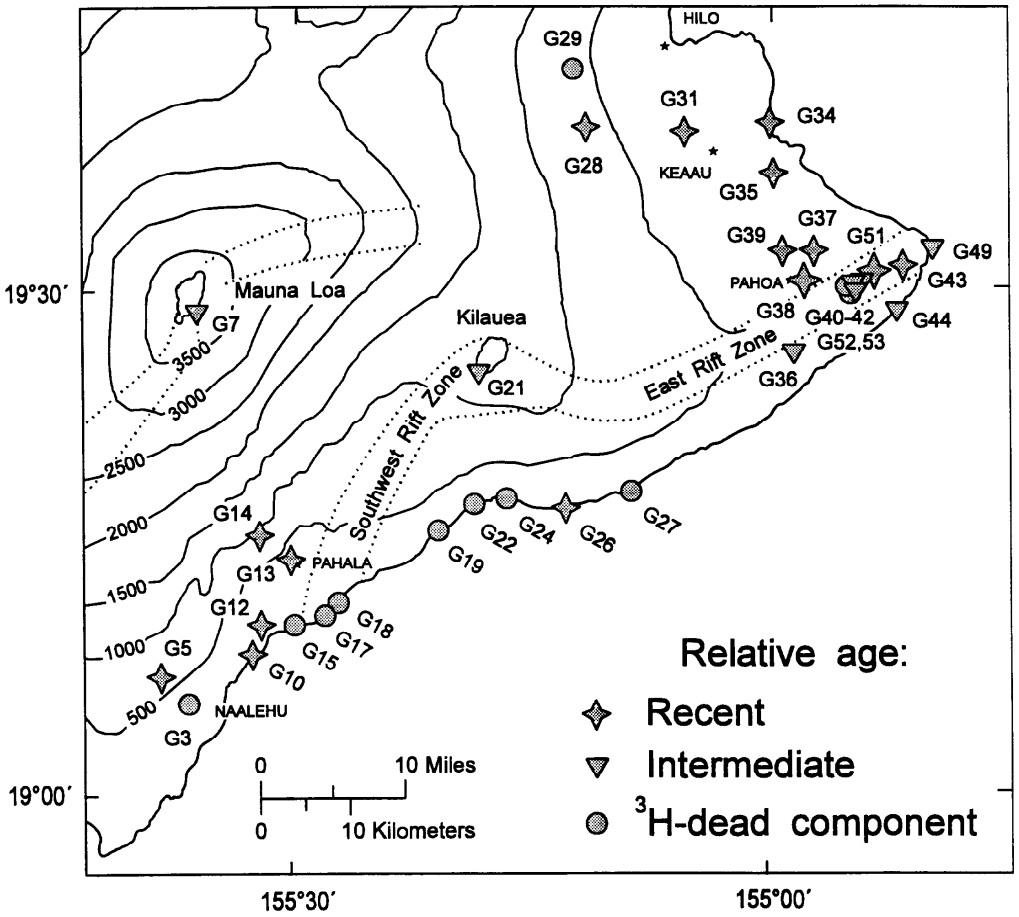

Figure 10. Relative age for ground water samples based on tritium content, after correction for seawater component.

Tritium

Tritium was measured in a subset of the ground-water samples to determine their relative age (table 3). As the ^3H levels do not vary substantially, the results are interpreted in a very general way. Residence times were estimated by comparing ^3H concentrations in the samples to the expected concentrations obtained by solving equations for two simple models of the flow system; the well-mixed reservoir and piston-flow models (Yurtsever, 1983). The well-mixed reservoir model assumes that all inputs to the flow system immediately mix with previous inputs, and concentration in the outflow depends on the residence time in the reservoir. The piston-flow model assumes that inputs to the flow system traverse the flowpath without mixing. Neither model includes the possibility of mixing between two or more separate reservoirs. Age estimates obtained using these models are very approximate and cover a broad range, but are useful for categorizing the relative ages of water discharging at different localities.

Atmospheric levels of bomb ^3H in the tropics were substantially lower than

Table 3. Measured tritium values for ground water and age estimates obtained from the well-mixed (WM) and piston-flow (P) models, for selected ground water samples from the study area. (---) denotes tritium content above the maximum predicted by the well-mixed model.

ID	State well no.	Location	Tritium (TU) 1991	1992	1993	1994	1995	Estimated age (years) WM	P
G3	0335-01	Naalehu well	-0.3	0.0				>500	>40
G5	0537-01	Haao spring	2.9					6	13-16
G7		Ainapo crack		4.5				---	20-25
G10		Kawa spring	3.8	2.8				7-20	14-19
G12	0831-03	Ninole B well	3.0					7-8	13-16
G13	1229-01	Pahala well	3.4	3.0				9-10	14-16
G14	1331-01	Alili spring	2.1					1	3-8
G15		Crack near Kamehame hill	1.9	1.9				1 or >75	5-10
G17		Pueo spring	0.7	0.8				>100	>35
G18		Waiapele crack		1.0				>100	>35
G19		Puu Elemakule spring	0.9	0.3				>100	>40
G21	2317-01	Kilauea summit borehole			5.4			---	23
G22		Kaaha cracks		1.2				>100	>35
G24		Halape springs		1.4				>100	>35
G26		Apua point crack	2.4					<3	9-12
G27		Crack near Kaena Point			1.7			>40	9-13
G28		Waiakea stream at gauge	2.1					1	1-3
G29	4211-01	Olaa Flume spring	1.4					>40	>35
G31	3804-01	Keaau (Shipman) well	2.2					1 or >40	9-12
G34		Haena beach spring	2.8	2.4				1-7	13-16
G35	3588-01	Paradise Park well		2.9				8	14-17
G36	2487-01	Keauohana well	4.9	5.0	4.8			---	19-25
G37	3185-01	Hawaiian Beaches well	2.5	3.7				<3	12-20
G38	2986-01	Pahoa 2A well	3.4	3.3				10-12	14-17
G39	3188-01	Keonepoko Nui well	2.8					6	13-16
G40	2983-01	PGV MW-1 well	4.2	3.7			3.5	---	18-22
G41	2883-07	PGV MW-2 well		3.8				---	18-20
G42	2983-02	PGV MW-3 well		4.2				---	18-20
G43	3080-01	Kapoho crater well	3.1	2.7				7-8	13-17
G44		Pohoiki spring		3.8				---	18-20
G49		Lighthouse spring		4.1				---	18-20
G51	2982-01	GTW-3 well		2.3				1-3	12-13
G52		KS-9 well					0.4	>100	>40
G53		KS-10 well					0.2	>100	>40
		Pohoiki seawater			1.6				
		Ka Lae seawater				1.5			
		Storm rain, Kona				2.0			
		Rainfall, P46, 8/93-2/94				2.4			
		Rainfall, P28, 8/93-2/94				2.0			
		Rain, shallow ground water*	2.4						

*from Goff et al., 1991

at higher latitudes in the northern hemisphere; ^3H levels in rainfall in Hawaii, at their maximum in 1963, were about 200 TU, 10 times less than at Ottawa, Canada. Levels of ^3H in rainfall were monitored by the IAEA at Hilo from 1962-69 and at Midway Island from 1962-84. The rest of the input record was estimated by correlation with Ottawa levels and several later values for Hawaii. Recent rainfall samples from the study area (Goff and others, 1991; this study, 1994) had a ^3H content of 2.0 - 2.4 TU, and ground-water samples ranged from 0 to 5.4 TU (table 3). Samples were analyzed at the 0.25 TU precision level.

Coastal spring samples and well samples were corrected to an apparent freshwater ^3H content by assuming seawater ^3H content of 1.6 TU, although ^3H in seawater in the inland wells may have been much lower. These corrections were not significant for less than 10 percent seawater. For 10 of 12 sites sampled two years in a row, similar residence times were obtained for both samples. Ground-water samples were divided into 3 categories according to apparent age: 1) older waters, with ^3H significantly less than recent rainfall, 2) intermediate-age waters, with ^3H significantly higher than recent rainfall, and 3) recent waters, with ^3H content close to recent rainfall. Waters with less than 1.8 TU were assumed to have been recharged more than 35 years ago or to be a mixture of recent rainfall and tritium-dead water. Waters with greater than 3.5 TU were assumed to be of intermediate age, with approximately 18-25 year residence time. Waters with ^3H content between 1.8 and 3.5 TU were assumed to be relatively recent rainfall, with 0-17 year residence time. Age estimates based on the well-mixed and piston-flow models are listed in table 3 and shown in figure 10.

INTERPRETATION OF GROUND-WATER HYDROLOGY

General Considerations in Interpretation of Ground-water Samples

The isotopic composition of most of the coastal springs to the north and the west of Kilauea's rift zones suggests that the coastal ground-water discharge represents flow from relatively large distances upslope, rather than local recharge (table 2, fig. 11). Theory indicates that discharge from a ground-water lens to the ocean occurs at the freshwater/saltwater interface, either inland above sea level or along the land surface extending below sea level (for example Cooper and others, 1964). Flowpaths converge at the discharge point, with local recharge presumably discharging at a higher elevation along the water table and recharge from far upslope discharging lower, possibly below sea level. The springs in the study area were sampled at or slightly above sea level, and the isotopic data suggest that the sample is a mixture of flowpaths. On Hawaii, unlike Oahu and other older islands in the Hawaiian chain, there is no low-permeability caprock of coral deposits between the ocean and the high-permeability basalts inland. Tidal fluctuations account for most of the mixing in salt-water/freshwater transition zones (Cooper and others, 1964; Underwood and others, 1992) and may explain the apparently well-mixed nature of the coastal discharge.

Isotopic composition of ground water from wells in the area also may represent recharge from various distances upslope. The wells sample the interval of the basal lens penetrated by the uncased or perforated portion of the well. For the (relatively few) wells sampled in this study, there is no clear relation between the length of the water column in the well and the calculated recharge elevation.

Compartmentalization of Regional Ground-water System by Rift Zones

Estimated recharge elevations for ground water in the study area (fig. 11) indicate that the rift zones of Kilauea effectively compartmentalize the ground-water system, dividing it into distinct hydrogeologic subareas. A brief description of each subarea and discussion of the isotopic results follows, going from south to north along the coast.

West of Kilauea's Southwest Rift Zone

The surface topography of the area from Naalehu to Pahala, west of the SWRZ, is characterized by fault scarps and highly eroded, steep-sided valleys that are surrounded by hills which appear to be upthrown fault blocks of much older flows (Lipman, 1980). The subsurface geology in the area likely consists of basalt flows over fault scarps, these and fault-driven realignment of low-permeability layers (ash, soil or dense flow bottoms) with permeable flow tops probably result in a heterogeneous permeability structure. Stable isotopes in precipitation in the mid-slope band of high rainfall follow the tradewind gradient with elevation, whereas near sea level (P9, P10) the precipitation isotopes fall into the rain-shadow group (figs. 4,7). The ground-water isotope data in this area (sites G1-G12, and 14 from McMurtry and others (1977)) show variable recharge elevations. Relatively enriched $\delta^{18}O$ values were found in the middle of the area (G3, 14 and G10), suggesting recharge from the high-rainfall area. Other samples down-gradient of the high rainfall area (G11, G12) have more depleted isotopic content. Although calculated maximum recharge elevations for some of the springs and wells in this area were higher, the flow-paths as drawn in figure 11 end at Mauna Loa's SWRZ, which is assumed to be a ground-water divide.

South of Kilauea's summit and East Rift Zone

The area south of Kilauea summit is entirely within Hawaii Volcanoes National Park. There are no wells near the shoreline, and samples of ground water are available only from coastal springs and cracks. Geophysical measurements suggest a body of impounded water in the summit area and in the upper portion of both rift zones (Jackson and Kauahikaua, 1987, 1990; fig. 1), and are compatible with data from a well near Kilauea Crater (G21), in which water levels have ranged from 611 to 633 m above sea level (Keller and others, 1979; Tilling and Jones, 1995). Kilauea summit and the area to the south straddles the boundary between the tradewind rainfall to the east and the rain shadow (figs. 2, 7A), with rainfall decreasing from 1,500 to less than 750 mm/year from northeast to southwest. Recharge elevations for most of the coastal springs south of Kilauea summit (G19-G25) were calculated using the precipitation/

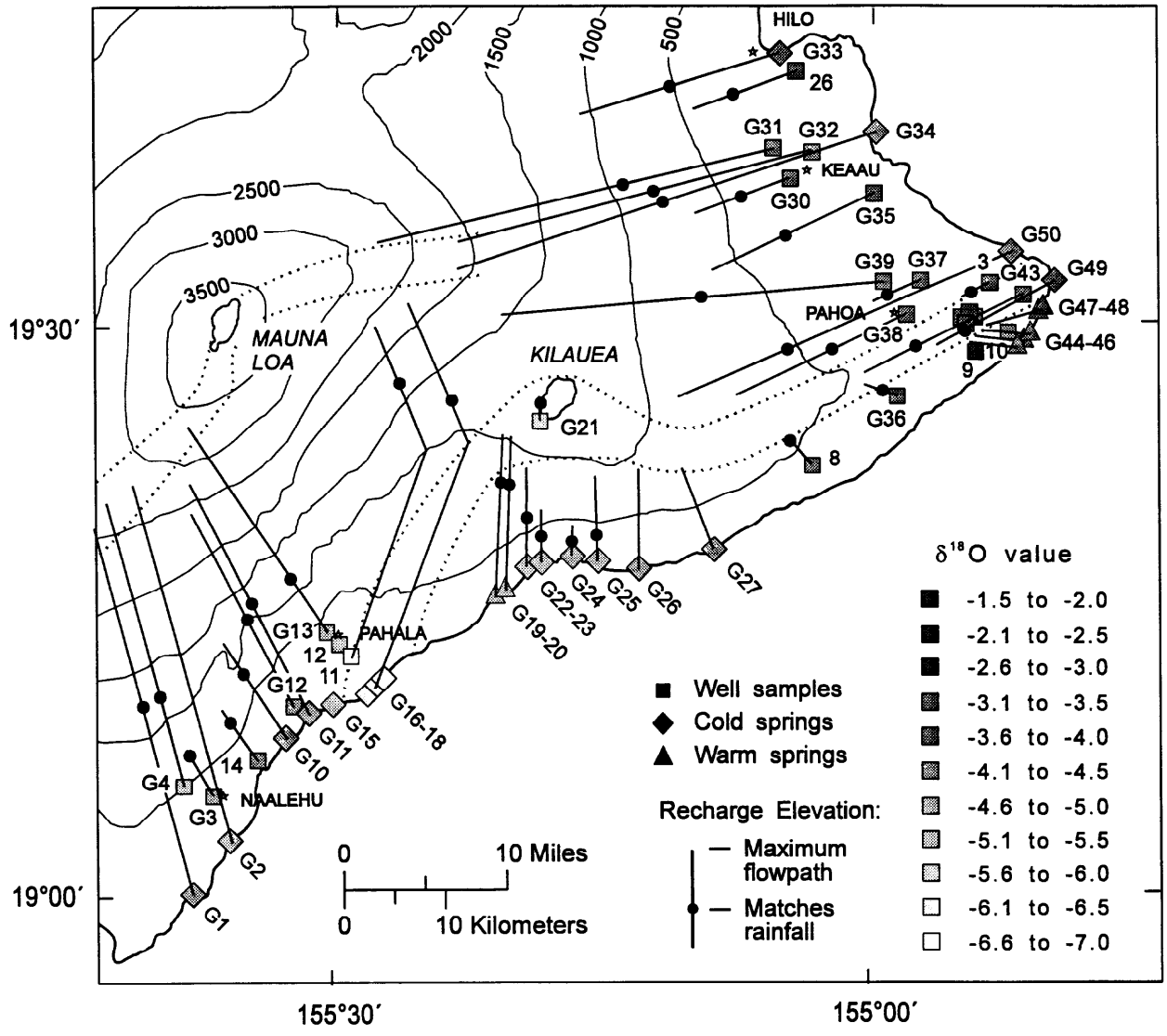

Figure 11. Calculated recharge elevations for the study area. Where both ^{18}O and D were used to calculate recharge elevations, the highest elevation is shown. Stable isotope data for sample sites 14, 11, 12, 8, 9, 10, 3, and 26 were published in McMurtry and others, 1977.

elevation relation for the rain shadow area. None of these coastal springs appear to be recharged at elevations above the summit and rift zones, and several of the springs appear to be recharged no higher than about 750 m elevation (fig. 11, table 2). The eastern-most springs in this area (G26, G27) are located such that both storm and trade-wind rainfall probably contribute to recharge. Their recharge elevation was calculated assuming that half the recharge comes from storms and half from tradewind rains. On this basis, recharge elevations for those two springs are also no higher than the rift zone. Wells and springs south of the ERZ (G36; 8-10 from McMurtry and others (1977),

and G44-49), had more enriched isotopic composition than those further west, and recharge elevation was calculated using the tradewind relation. Isotopic composition for these springs and wells also indicates that they are recharged locally.

North of Kilauea's East Rift Zone

The area north of Kilauea's ERZ (Pahoa to Hilo) includes the north flank of Kilauea and the eastern slope of Mauna Loa. This area is underlain by intercalated flows from Kilauea's ERZ and summit and Mauna Loa's northeast rift zone (Moore and Trusdell, 1993). Kilauea's ERZ is thought to have moved southward over time, and gravity measurements imply the presence of buried dikes to the north of the current surface trace of the rift (Swanson and others, 1976; Kauahikaua, 1993). The area generally faces east-northeast toward the tradewinds, and receives the highest rainfall in the study area (figs. 2 and 4). Precipitation isotopes all follow the tradewind relation with elevation (fig. 7). The stable isotope composition of the ground water generally matches that of precipitation within a midslope area of maximum rainfall (4,000 mm per year and higher) at about 250-1250 m elevation (fig. 2), although some of the calculated flow paths for integrated recharge extend much higher (G31-G32, G34, G39).

Compartmentalization by Rift Zones

The stable isotope data for the entire study area strongly indicate that the area south of Kilauea's rift zones is isolated from flow systems north and west of Kilauea summit and rift zones. It had previously been recognized that Kilauea's lower ERZ probably forms a barrier to southward movement of ground water (Davis and Yamanaga, 1968; Druecker and Fan, 1976). The data reported here indicate that the area south of the SWRZ, Kilauea summit, and the upper ERZ is also hydraulically isolated. This supports Takasaki's (1993) hypothesis that the entire regional flow system is compartmentalized by the rift zones of Kilauea.

The tritium data also support the hypothesis that the rift zones compartmentalize the regional ground-water system. In general, the older and intermediate-age waters are within or downgradient of the rift zones, while ^{3}H content of all but two of the ground-water samples in areas outside the rift zones falls into the recent recharge category (fig. 10). Tritium content for all the coastal springs south of Kilauea summit, except G26, is lower than that of recent rainfall, suggesting that the water discharging at the coast is a mixture of recent rainfall and water recharged more than 35 years ago (tritium-dead water). Although rainfall in the area is low compared to the rest of the island, it is still relatively high (750-1,500 mm per year) and recharge is probably substantial, since the highly permeable young basalts are sparsely vegetated. Travel times for ground water in that area may not be long enough to account for the tritium-dead water. The high-level, impounded water in the summit area seems a more plausible source for a tritium-dead component in the spring discharge.

Another area where tritium-dead water may signal the leakage of impounded water is the Naalehu well (G3), which

had the oldest water sampled in the study (0 TU), and a water level of 3 m, as expected for a basal lens. The nearby Waiohinu exploratory well (G4) at 396 m elevation had a water level of 310 m (W. Meyer, USGS Honolulu, written comm., 1995), and there are high-elevation springs uphill from the Naalehu well, suggesting that there is a low-permeability feature impounding water upgradient. Leakage of water that had been impounded could account for the greater age of the water in the Naalehu well.

Down-rift Ground-water Flow: SWRZ Versus ERZ

The western boundary between Kilauea and Mauna Loa runs approximately parallel to the trace of the SWRZ. As is the case with the ERZ, gravity measurements indicate that the active rift zone has moved south or seaward over time (Swanson and others, 1976; Kauahikaua, 1993), and we assume that there are buried dikes extending some distance north and west of the current surface trace of the rift zone. The lower part of the SWRZ lies downslope from the area of relatively high, isotopically enriched rainfall above Pahala and Naalehu (fig. 2). In contrast, the sparse rainfall over the upper part of the SWRZ has the depleted isotopic composition of the rain-shadow area (fig. 7). Four coastal springs (G15-18) and three Pahala-area wells (11, 12, G13) are considered to be within or influenced by the SWRZ structure (fig. 11).

Initial water levels in the three wells near Pahala (G13, 12, and 11; drilled in 1974, 1947, and 1970, respectively) were 117 m, 70 m and 3 m above sea level, corroborating earlier suggestions (Hussong and Cox, 1967; Adams and others, 1970) that low-permeability barriers impound ground water in well 12. The 57 m difference in water level between wells 12 and G13, over a distance of less than 2 km, further suggests that there may be a series of barriers parallel to the SWRZ. Isotopic composition of ground water shows a transition from relatively isotopically enriched water at G13 ($\delta^{18}O$ = -4.7), compatible with recharge from the tradewind rainfall area, to isotopically depleted water at 11 and the coastal springs directly downslope (G16-G18, $\delta^{18}O$ = -6.3 to -6.7). The coastal springs show an isotopic transition across the rift zone boundary (from G11 to G15 to G16-G18) that is similar to the transition observed in the wells (G13 to 12 to 11). Tritium in the SWRZ coastal springs (G16, G18) was significantly lower than rainfall, suggesting the springs discharge a mixture of recent recharge with water that has been in the system more than 35 years, whereas tritium in well G13 indicated relatively recent recharge (fig. 10). The transition in isotopic content for ground water in the area can be explained by a series of dikes or buried fault scarps along the trend of the SWRZ that act as leaky barriers.

The isotopic evidence in the SWRZ indicates that 1) recharge from the midslope high-rainfall area is blocked from discharging at the shoreline in the rift zone and 2) water discharging at the SWRZ springs is recharged somewhere above 1,500 m. The coastal spring water (G16-G18) is more isotopically depleted than that found in the well near Kilauea summit (G21) and is not heated, suggesting that it enters the upper part of the

rift zone from the slopes of Mauna Loa and travels through an older or inactive portion of the rift zone.

The East Rift Zone of Kilauea is an area of particular hydrologic interest, as the geothermal fluids in the lower ERZ have been produced for electrical power generation and there has been geothermal exploration in other areas along the rift zone. The entire ERZ is within the tradewind rainfall area, and rainfall is uniform at 3,000 mm/year along most of the length of the rift (fig. 2). There are no wells in the upper ERZ, and wells (for example well 8) and coastal springs that once existed below the middle section of the rift have been covered by recent (1983-present) lava flows from vents in the mid- to upper ERZ. Samples obtained for this study were predominantly from coastal warm springs and shallow wells in the lower ERZ (fig. 4).

Apparent recharge elevations for ground water in this area are fairly ambiguous. Volume-weighted average precipitation $\delta^{18}O$ and δD did not vary significantly between the 2 collectors at 0 and 370 m elevation along the rift zone (P59: -3.6, -17; P51: -3.6, -15), although the regression on all tradewind data (fig. 7) predicts a 0.6 per mil difference in $\delta^{18}O$. Within and south of the lower ERZ, stable isotope composition of ground-water samples was either similar to or more enriched than local rainfall. Unlike the SWRZ, there is no evidence from the shallow wells and springs to support the idea of down-rift flow from the vicinity of Kilauea summit. Flow from middle elevations on the rift zone (about 628 m elevation) would have to comprise greater than 20 percent of the sample to be detectable. All of the wells we measured in this area were in the shallow ground-water system (no more than 40 m below sea level); isotopic composition of water from deeper wells, which we were unable to sample satisfactorily, might show evidence of down-rift flow.

The two wells (G37, G38) and a coastal spring (G50) immediately north of the current surface expression of the ERZ have calculated maximum recharge elevations that do not extend as far as Kilauea summit (fig. 11). It is possible that ground-water flow in this area is affected by buried dikes in the older part of the rift, or that flow further upslope is restricted by the northward bend of the current upper ERZ. Chemistry of the Pahoa well (G38) shows elevated sulfate levels, suggesting input of water affected by magmatic gases (Janik and others, 1994).

Tritium measured in the samples from the ERZ, with two exceptions (G43, approximately 2 m deep, and G51), indicated intermediate to old waters. Tritium content in most shallow wells and coastal springs in the lower ERZ was significantly higher than in ground water to the north of the ERZ and in rainfall. Tritium in the deep geothermal wells (G52, G53) was very low. Thus water in and south of the lower ERZ has a longer residence time than waters north of the rift. Since the freshwater stable isotopes do not indicate down-rift flow of ground water, low-permeability dikes in the rift may contribute to longer residence time by impeding outflow. Thermally driven convective circulation within and near the rift zone may also contribute older, deeper water to the springs and shallow wells.

Isotopic Enrichment in Thermal Waters

Ground water sampled in the area south of Kilauea's rift zones and summit is warmer than ground water sampled in other parts of the study area. Average temperatures in coastal springs and cracks downgradient of the summit and rift zones ranged from 24-39°C, whereas coastal spring temperatures west and north of the rift zones ranged from 18-22°C.

The warm springs downgradient from the lower ERZ do not contain thermal fluids like those found in the deep geothermal wells in the rift zone. Rather, their chemistry is that of diluted seawater except for silica and bicarbonate levels, and silica and chloride content increase with increasing temperature. A plausible explanation for the spring chemistry is that seawater in saturated rock below the freshwater lens south of the lower ERZ is heated to about 165°C, boils to 100°C and loses steam, and then mixes with the overlying freshwater lens and flows toward the shoreline, where it is further mixed with seawater from the ocean as it discharges (Janik and others, 1994).

Many of the warm springs south of the lower ERZ had δD or $\delta^{18}O$ values, after correcting for seawater content, that were slightly more enriched than local rainfall; this might be expected for ^{18}O, if there was some exchange with rock, but not for D. The shallow monitoring wells (G40-G42) on the lower ERZ also had isotopic contents more enriched than local rainfall. Possible explanations are: 1) boiling of the near-rift seawater end-member resulted in an isotopic composition more enriched than the seawater value (δD and $\delta^{18}O$ = 0 per mil) which we used as the correction; 2) data were not sufficient to define a long-term rainfall average for the area; and 3) there was vapor loss from the heated water through the unsaturated zone along the flowpath. Recharge of the freshwater component for the warm springs and wells was assumed to be local (fig. 11), but factors other than elevation of recharge could be influencing isotopic composition in those samples.

Stable isotopes in the coastal springs south of Kilauea summit (G22-G25) are also enriched relative to upslope rainfall. Isotopic composition of rainfall over Kilauea summit is quite variable across the tradewind/rain shadow boundary, with volume-weighted average $\delta^{18}O$, δD varying from (-4.6, -22) to (-5.1, -29) to (-6.3, -38) over a small (15 km^2) area at sites P26, P28, and P24 (fig. 4). Stable isotopes measured in well G21 near the summit (-5.6, -32) are close to the average of the two nearest rain collectors (P24, P28), so ground water in the summit area appears to be somewhat more isotopically enriched than precipitation falling downslope in the rain-shadow area (average $\delta^{18}O$, δD of -6.0, -37; P20-P22). Isotopic composition of rainfall measured in collectors at the coast ranged from (-4.1, -25) at P23 on the east to (-5.0, -31) at P10 on the west.

This presents a problem in interpretation, because 1) the coastal groundwater samples are more isotopically enriched than the average rainfall immediately upslope, and are most similar to either coastal rainfall or Kilauea summit rainfall, and 2) the ^{3}H data and elevated temperature suggest that the coastal springs south of Kilauea summit contain

a component of impounded ground water from the summit area. Perhaps there is some degree of thermal stratification, where warm water leaking from the summit area floats on the top of the freshwater lens, as was noted by McMurtry and others (1977) for a well in the lower ERZ. Despite tidal mixing near the coast, some thermal stratification may be preserved, so that the samples taken at sea level in the cracks and springs contain a larger portion of thermal water.

SUMMARY

Significant areal differences in precipitation isotopes on the Island of Hawaii correlate strongly with general climatological patterns. High rainfall areas have frequent rains due to the orographic lifting of moist air carried by the tradewinds or by a thermally-driven seabreeze cycle. The isotopic content of cumulative samples from these high-rainfall areas agrees well with that predicted from first-stage condensation of atmospheric vapor above the ocean, and precipitation isotopes get more depleted with increasing elevation and distance inland, as expected, due to decreasing temperature and rainout effects. In areas of lower rainfall, most rainfall occurs during storms. For the area in the rain shadow of Kilauea volcano, isotopic content of precipitation samples also varies with elevation and distance inland, but is more depleted than at corresponding elevations in the tradewind areas. The depleted isotopic composition of precipitation in the rain shadow can be explained by the processes affecting rainfall there. Although the original source of vapor in storms is the oceanic atmosphere, condensation temperatures for large storms are generally lower and such storms are often raining before they reach the island. For the high-elevation area above the orographic rainfall influence, precipitation isotopes also vary with elevation, but the rate of decrease in δ-values with elevation is greater than for lower-elevation areas, presumably due to the difference in isotopic fractionation factors when condensation temperatures are below 0 to -15°C.

It seems reasonable to expect that similar relations between precipitation isotope content and elevation may apply to other islands, and possibly coastal continental areas at similar latitudes. In particular, the other Hawaiian Islands have very similar temperature lapse rates and climatological patterns. It may be feasible to use stable isotopes as tracers for ground-water flow on the other islands with fewer precipitation samples, just sufficient to establish that gradients are similar. However, this study also underscores the importance of a collection strategy that takes areal variations in rainfall patterns into account, as precipitation isotopes vary significantly with microclimates.

Stable isotopes worked well as tracers of ground-water flowpaths in the southeast part of the Island of Hawaii. The lower levels of atmospheric bomb ^{3}H in the southern part of the hemisphere made it a less useful age-dating tool than in northern latitudes, but it was possible to distinguish broad age categories for ground water in the study area. The isotope data establish that Kilauea's rift zones effectively compartmentalize the ground-water system, with relatively local recharge and longer residence times for ground water in and downgradient of

the rift. The isotope data also show that the impounded water near Kilauea summit is recharged locally. Some heated ground water from the summit area may leak southward to the springs at the shoreline. Both stable isotope and tritium data indicate that part of Kilauea's SWRZ acts as a conduit for ground-water flow, and suggest that rift-zone dikes separate ground-water flow systems in the Pahala area. Stable isotopes from the shallow wells and thermal springs in the lower ERZ showed no evidence for down-rift flow. Therefore, elevated ^{3}H levels in the lower ERZ shallow ground water suggest low permeabilities, rather than a long flowpath.

REFERENCES

Adams, A.I., Goff , F. and Counce, D., 1995, Chemical and isotopic variations of precipitation in the Los Alamos region, New Mexico: Los Alamos National Laboratory Report LA-12895-MS, UC-903, 35 p.

Adams, W.M., Mathur, S.P., and Huber, R.D., 1970, Aeromagnetic, gravity, and electrical resistivity exploration between Pahala and Punaluu, Hawaii: Hawaii Institute of Geophysics Technical Report 28, 62 p.

Blumenstock , D.I., and Price, S., , 1967, Climates of the states: Hawaii, *in* Climatography of the United States: no. 60-51, U.S. Dept. of Commerce, Washington, D.C.

Climatological Data, Hawaii and Pacific, February 1992 through August 1994, National Oceanic and Atmospheric Administration, National Climatic Data Center, Asheville, N.C.

Cooper, H.H., Kohout, F.A., Henry, H.R., and Glover, R.E., 1964, Sea water in coastal aquifers - relation of salt water to fresh ground water: U.S. Geological Survey Water-Supply Paper 1613-C, 84 p.

Craig, H., 1961, Isotopic variations in meteoric waters: Science, v. 133, p. 1702-1703.

Craig, H. and Gordon, L.I., 1965, Deuterium and oxygen 18 variations in the ocean and the marine atmosphere, *in* Tongiorgi, E., ed., Stable Isotopes in Oceanographic Studies and Paleotemperatures: Spoleto Conference in Nuclear Geology, Italian National Council of Research and University of Pisa, p. 9-130.

Dansgaard, W., 1964, Stable isotopes in precipitation: Tellus, v. 16, no. 4, p. 436-468.

Davis, D.A., and Yamanaga, George, 1968, Preliminary report on the water resources of the Hilo-Puna area, Hawaii: Hawaii Division of Water and Land Development, Dept. of Land and Natural Resources Circular C45, 38 p.

Druecker, M., and Fan, P., 1976, Hydrology and chemistry of ground water in Puna, Hawaii: Ground Water, v. 14, no. 5, p. 328-338.

Ekern, P.C., and Chang, J.-H., 1985, Pan evaporation: State of Hawaii, 1894-1983: Hawaii Division of Water and Land Development, Dept. of Land and Natural Resources Report R74, 171 p.

Eyre, P., Ewart, C., and Shade, P., 1986, Hydrology of the leeward aquifers, southeast Oahu, Hawaii: U.S. Geological Survey Water-Resources Investigations Report 85-4270, 75 p.

Fischer, W.A., Davis, D.A., and Sousa, T.M., 1966, Fresh-water springs of Hawaii from infrared images: U.S. Geological Survey Hydrologic Investigations Atlas HA-218, 1 sheet.

Fontes, J. Ch., 1980, Environmental isotopes in groundwater hydrology, *in* Fritz, P. and Fontes, J. Ch., eds., Handbook of Environmental Isotope Geochemistry, v. 1, The Terrestrial Environment: Elsevier, Amsterdam, p. 74-134.

Friedman, I., Smith, G.I., Gleason, J.D., Warden, A., and Harris, J.M., 1992, Stable isotope composition of waters in southeastern California, 1. Modern precipitation: Journal of Geophysical Research, v. 97, no. D5, p. 5795-5812.

Friedman, I., and Woodcock, A.H., 1957, Determination of deuterium-hydrogen ratios in Hawaiian waters: Tellus, v. 9, no. 4, p. 553-556.

Gat, J.R., 1971, Comments on the stable isotope method in regional groundwater investigations: Water Resources Research, v. 7, no. 4, p. 980-993.

Gat, J.R., and Dansgaard, W., 1972, Stable isotope survey of the fresh water occurrences in Israel and the northern Jordan Rift Valley: Journal of Hydrology, v. 16, p. 177-212.

Gat, J.R., Bowser, C.J., and Kendall, C., 1994, The contribution of evaporation from the Great Lakes to the continental atmosphere: estimate based on stable isotope data: Geophysical Research Letters, v. 21, no. 7, p. 557-560.

Giambelluca, T.W., Nullet, M.A., and Schroeder, T.A., 1986, Rainfall atlas of Hawaii: Hawaii Division of Water and Land Development, Dept. of Land and Natural Resources Report R76, 267 p.

Giambelluca, T.W. and Sanderson, M., 1993, The water balance and climatic classification, *in* Sanderson, M., ed., Prevailing Trade Winds, Weather and Climate in Hawaii: University of Hawaii Press, Honolulu, p. 56-72.

Goff, F., McMurtry, G.M., and Adams, A.I., 1991, Deuterium, tritium and oxygen-18 in meteoric, geothermal and magmatic waters at Kilauea Volcano, Hawaii [abs.]: EOS Transactions of the American Geophysical Union, v. 72, no. 44, p. 558.

Gonfiantini, R., 1978, Standards for stable isotope measurements in natural compounds: Nature, v. 271, p. 534-536.

Hsieh, J.C.C., Savin, S.M., Chadwick, O.A., and Kelly, E.F., 1994, Soil genesis along an arid to humid climate transect in Hawaii, II. Water and pedogenic mineral oxygen isotope relationships [abs.]: Geological Society of America Abstracts with Programs, 1994 Annual Meeting, v. 26, no. 7, p. A-88.

Hussong, D.M., and Cox, D.C., 1967, Estimation of ground-water configuration near Pahala, Hawaii, using electrical resistivity techniques: University of Hawaii Water Resources Research Center Technical Report 17, 35 p.

International Atomic Energy Agency, 1953-1975, Environmental Isotope Data: World Survey of Isotope Concentration in Precipitation: International Atomic Energy Agency (IAEA) Technical Report Series, nos. 96, 117, 129, 147, 165, and 192.

Ingebritsen, S.E., and Scholl, M.A., 1993, The hydrogeology of Kilauea volcano: Geothermics, v. 22, no. 4, p. 255-270.

Ingebritsen, S.E., Mariner, R.H., and Sherrod, D.R., 1994, Hydrothermal systems of the Cascade Range, north-central Oregon: U.S. Geological Survey Professional Paper 1044-L, 86 p., 2 pls.

Ingraham, N.L., and Craig, R.G., 1993, Constraining estimates of evapotranspiration with hydrogen isotopes in a seasonal orographic model, *in* Climate change in continental isotopic records: Geophysical Monograph 78, American Geophysical Union, p. 47-53.

Ingraham, N.L., and Taylor, B.E., 1991, Light stable isotope systematics of large-scale hydrologic regimes in California and Nevada: Water Resources Research, v. 27, no. 1, p. 77-90.

Jackson, D.B., and Kauahikaua, J., 1987, Regional self-potential anomalies at Kilauea Volcano, *in* Decker, R.W., Wright, T.L., and Stauffer, P.H., eds., Volcanism in Hawaii: U.S. Geological Survey Professional Paper 1350, p. 947-959.

Jackson, D.B., and Kauahikaua, J., 1990, The high-level water table beneath Kilauea Volcano, Hawai'i [abs.]: EOS Transactions of the American Geophysical Union, v. 71, no. 43, p. 1676.

Janik, C.J., Nathenson, M., and Scholl, M.A., 1994, Chemistry of spring and well waters on Kilauea Volcano, Hawaii, and vicinity: U.S. Geological Survey Open-File Report 94-586, 166 p.

Kauahikaua, J., 1993, Geophysical characteristics of the hydrothermal systems of Kilauea Volcano, Hawaii: Geothermics, v. 22, no. 4, p. 271-299.

Keller, G.V., Grose, L.T., Murray, J.C., and Skokan, C.K., 1979, Results of an experimental drillhole at the summit of Kilauea volcano, Hawaii: Journal of Volcanology and Geothermal Research, v. 5, p. 345-385.

Kendall, C., 1992, Temporal, spatial and species effects on the oxygen and hydrogen isotopic compositions of throughfall [abs.]: EOS Transactions of the American Geophysical Union, v. 73, no. 43, p. 160.

Kroopnick, P.M., Buddemeier, R.W., Thomas, D., Lau, L.S., and Bills, D., 1978, Hydrology and geochemistry of a Hawaiian geothermal system: HGP-A: Hawaii Institute of Geophysics Technical Report HIG 78-6, 64 p.

Lipman, P.W., 1980, The southwest rift zone of Mauna Loa: Implications for structural evolution of Hawaiian volcanoes: American Journal of Science, v. 280-A, p. 752-776.

Liu, K., 1984, Hydrogen and oxygen isotopic compositions of meteoric waters from the Tatun Shan area, northern Taiwan: Bulletin of the Institute of Earth Sciences, Academia Sinica, v. 4, p. 159-175.

McMurtry, G.M., Fan, P.F., and Coplen, T.B., 1977, Chemical and isotopic investigations of groundwater in potential geothermal areas in Hawaii: American Journal of Science, v. 277, p. 438-458.

Moore, R.B. and Trusdell, F.A., 1993, Geology of Kilauea volcano: Geothermics, v. 22, no. 4, p. 243-254.

Nullet, D., and Sanderson, M., 1993, Radiation and energy balances and air temperature, *in* Sanderson, M., ed., Prevailing Trade Winds, Weather and Climate in Hawaii: University of Hawaii Press, p. 37-55.

Salati, E., Dall'Olio, A., Matsui, E., and Gat, J.R., 1979, Recycling of water in the Amazon Basin: an isotopic study: Water Resources Research, v. 15, no. 5, p. 1250-1258.

Scholl, M.A., Ingebritsen, S.E., Janik, C.J., and Kauahikaua, J.P., 1992, Geochemical and stable-isotope composition of precipitation and groundwater, Kilauea volcano area, Hawaii - preliminary results [abs.]: EOS Transactions of the American Geophysical Union, v. 73, no. 43, p. 161.

Scholl, M.A., Janik, C.J., Ingebritsen, S.E., Kauahikaua, J.P., and Trusdell, F.A., 1993, Preliminary results from an isotope hydrology study of the Kilauea volcano area, Hawaii: Geothermal Resources Council Transactions, v. 17, p. 187-194.

Scholl, M.A., and Ingebritsen, S.E., 1995, Total and non-seasalt sulfate and chloride measured in bulk precipitation samples from the Kilauea volcano area, Hawaii: U.S. Geological Survey Water-Resources Investigations Report 95-4001, 32 p.

Schroeder, T.A., 1993, Climate controls, *in* Sanderson, M., ed., Prevailing Trade Winds, Weather and Climate in Hawaii: University of Hawaii Press, p. 12-36.

Smith, G.I., Friedman, I., Klieforth, H., and Hardcastle, K., 1979, Areal distribution of deuterium in eastern California precipitation, 1968-1969: Journal of Applied Meteorology, v. 18, p. 172-188.

Sorey, M.L. and Colvard, E.M., 1994, Potential effects of the Hawaii Geothermal Project on ground-water resources on the Island of Hawaii: U.S. Geological Survey Water Resources Investigations Report 94-4028, 35 p.

Souza, W.R., and Voss, C.I., 1987, Analysis of an anisotropic coastal aquifer system using variable-density flow and transport simulation: Journal of Hydrology, v. 92, p. 17-41.

Stearns, H.T., and Clark, W.O., 1930, Geology and water resources of the Kau District, Hawaii: U.S. Geological Survey Water-Supply Paper 616, 194 p.

Stearns, H.T., and Macdonald, G.A., 1946, Geology and ground-water resources of the Island of Hawaii: Hawaii Division of Hydrography Bulletin 9, 362 p.

Swanson, D.A., Duffield, W.A., and Fiske, R.S., 1976, Displacement of the south flank of Kilauea volcano: the result of forceful intrusion of magma into the rift zones: U.S. Geological Survey Professional Paper 963, 39 p.

Takasaki, K.J., 1993, Ground water in Kilauea Volcano and adjacent areas of Mauna Loa Volcano, Island of Hawaii: U.S. Geological Survey Open-File Report 93-82, 28 p.

Takasaki, K.J., and Mink, J.K., 1985, Dike-impounded ground-water reservoirs, Island of Oahu: U.S. Geological Survey Water-Supply Paper 2217, 77 p.

Tilling, R.I., and Jones, B.F., 1995, Composition of waters from the research drill hole at the summit of Kilauea volcano, Hawaii: 1973-1991: U.S. Geological Survey Open-File Report 95-532, 41 p.

Underwood, M.R., Peterson, F.L., and Voss, C.I., 1992, Groundwater lens dynamics of atoll islands: Water Resources Research, v. 28, no. 11, p. 2889-2902.

Yonge, C.J., Goldenberg, L., and Krouse, H.R., 1989, An isotope study of water bodies along a traverse of southwestern Canada: Journal of Hydrology, v. 106, p. 245-255.

Yurtsever, Y. and Gat, J.R., 1981, Atmospheric waters, *in* Gat, J.R. and Gonfiantini, R., eds., Stable Isotope Hydrology, Deuterium and Oxygen-18 in the Water Cycle: International Atomic Energy Agency (IAEA) Technical Reports Series No. 210, Vienna, p.103-143.

Yurtsever, Y., 1983, Models for tracer data analysis, *in* Guidebook on nuclear techniques in hydrology: International Atomic Energy Agency (IAEA) Technical Reports Series no. 91, 437 p.

Appendix 1. Precipitation collector site locations, collection periods, and isotopic composition of samples for the southeast part of the Island of Hawaii. Abbreviations: VWA: Volume-weighted average; HVNP: Hawaii Volcanoes National Park; Obs.: Observatory; UH Ag. Exp. Sta.: University of Hawaii Agricultural Experiment Station; SOH-4: State of Hawaii Scientific Observation Hole Number 4; IAEA: International Atomic Energy Agency; C of C: Chain of Craters; Rd: Road, R: River, Co: Company. Collection periods: 1: 2/92 to 9/92; 2: 9/92 to 3/93; 3: 3/93 to 8/93; 4: 8/93 to 2/94; 5: 2/94 to 8/94.

Site	Location	Elev-ation (m)	Long-itude	Lati-tude	Precipitation (mm)					$\delta^{18}O$ (‰)					δD (‰)					VWA	
					1	2	3	4	5	1	2	3	4	5	1	2	3	4	5	$\delta^{18}O$	δD
P1	Ka Lae	6	155.670	18.920		413		398			-4.2		-4.1			-24		-28		-3.4	-16[c]
P2	South Point Road	475	155.660	19.044	494		468[†]			-3.5		-2.4[†]			-18		-4[†]				
P3	Kahuku Ranch	1292	155.703	19.141		470	374				-6.2	-3.6				-40	-14			-5.1	-28
P4	Kahuku Ranch	1594	155.686	19.178	588	380	340			-5.2	-7.0	-4.5			-32	-46	-22			-5.9	-36
P5	Kahuku Ranch	1884	155.633	19.232		411	507				-7.3	-4.7				-48	-23			-5.9	-34
P6	Kahuku Ranch	2201	155.575	19.306	621	394				-6.6	-8.6				-42	-58				-7.4	-48
P7	Mountain House Road	780	155.585	19.154	809	771[†]	764	570[†]	1362[§]	-2.5	-5.3[†]	-2.7	-5.1[†]	-4.7[§]	-9	-29[†]	-6	-29[†]	-24[§]	-4.2	-20
P8	Old Plantation Spring Rd.	686	155.617	19.108	761	533[†]	775			-2.8	-4.1[†]	-2.7			-9	-19[†]	-6			-3.3	-12
P9	Highway 11 at Punaluu	101	155.514	19.152		503[†]	253				-5.3[†]	-2.4				-34[†]	-6			-4.3	-24
P10	Palima Point	24	155.460	19.155	268	717				-3.4	-5.6				-20	-35				-5.0	-31
P11	Waiwelawela Point	21	155.389	19.202		693					-5.6					-35					
P12	Highway 11 at Kapapala	616	155.431	19.277	349	699	385[†]	290[†]		-4.7	-6.0	-3.2[†]	-6.2[†]		-27	-39	-12[†]	-41[†]		-5.0	-30
P13	Ainapo Trail[‡]	1524	155.458	19.375	2169[§]					-5.2[§]					-31[§]					-5.2	-31
P14	Ainapo Trail[‡]	2069	155.502	19.380	1146					-6.8					-41					-6.8	-41
P15	Ainapo Trail[‡]	2804	155.533	19.401	741[§]					-8.8[§]					-59[§]					-8.8	-59
P16	Ainapo Trail	3926	155.579	19.439	325	247[†]				-12.0	-13.3[†]				-85	-91[†]				-12.6	-88
P17	N of Mokuaweoweo	3974	155.581	19.471	243	232[†]				-12.4	-14.1[†]				-91	-100[†]				-13.2	-95
P18	Mauna Loa Slope Obs.	3401	155.578	19.537	321	251[†]	140[†]			-10.3	-13.8[†]	-10.4[†]			-71	-100[†]	-74[†]			-12.2	-87
P19A	Hwy 11 at Kau Trail	927	155.369	19.373	1700	906	318	485	688	-3.3	-7.4	-3.8	-6.1	-8.3	-17	-47	-16	-36	-59	-5.7	-34
P19B	Hwy 11 at Kau Trail	927	155.369	19.373	220					-4.4					-25						
P20	W Hilina Pali trailhead	634	155.322	19.293		1171	411[†]	492[†]	664		-6.4	-3.4[†]	-6.7[†]	-7.2		-40	-16[†]	-43[†]	-49	-5.9	-37
P21	Mauna Iki Trail	951	155.314	19.358	454	730[*]	265[†]			-4.7	-7.3	-3.9[†]			-29	-47	-23[†]			-6.4	-40
P22	Kipuka Nene Road	969	155.274	19.344		1135[†]	362				-6.2[†]	-3.6				-39[†]	-18			-5.6	-34
P23	Keahou Shelter, HVNP[‡]	24	155.233	19.272	895					-4.1					-25					-4.1	-25

Site	Location	Elev-ation (m)	Long-itude	Lati-tude	Precipitation (mm)					$\delta^{18}O$ (‰)					δD (‰)					VWA	
					1	2	3	4	5	1	2	3	4	5	1	2	3	4	5	$\delta^{18}O$	δD
P24	S of Halemaumau	1056	155.282	19.401		953	407				-7.4	-3.7				-48	-16			-6.3	-38
P25A	Crater Rim & C. of C. Rd.	1134	155.255	19.406	666		619			-3.8		-3.6			-18		-15				
P25B	Crater Rim & C. of C. Rd.	1134	155.255	19.406	648					-3.9					-19						
P26	Thurston Lava Tube	1195	155.238	19.416	1775	1183	1038			-3.6	-5.9	-3.5			-14	-32	-14			-4.6	-22
P27	Jade Road, Volcano	1079	155.218	19.433	1781					-3.1					-13						
P28	Hawaiian Volcano Obs.	1244	155.289	19.422	1727	871	382	2185	2087	-3.9	-6.8	-4.1	-4.8	-5.5	-21	-44	-18	-26	-35	-5.1	-29
P29	Kilauea Crater	1088	155.272	19.411	524					-3.1					-15						
P30	HVNP Headquarters	1207	155.261	19.432	771					-3.6					-17						
P31	Mauna Loa Road	1231	155.309	19.443	368	657	366			-3.8	-7.4	-4.2			-21	-48	-22			-6.2	-39
P32	UH Ag. Exp. Sta., Volcano	1244	155.261	19.476	938	1242				-3.9	-6.5				-19	-40				-5.3	-31
P33A	Mauna Loa Road	1493	155.342	19.462		998	488	1923	2300		-7.9	-5.0	-6.3	-7.1		-52	-26	-39	-45	-6.4	-40
P33B	Mauna Loa Road	1524	155.351	19.461	1337					-2.1					-12						
P33C	Mauna Loa Road	1524	155.351	19.461	205					-4.5					-28						
P34	Mauna Loa trailhead	2034	155.387	19.495	455	900				-5.2	-8.3				-33	-54				-7.2	-47
P35	Mauna Loa trail	2438	155.409	19.517	385	686	422	1099	3266[§]	-6.4	-9.5	-6.5	-9.0	-8.8[§]	-41	-63	-38	-59	-58[§]	-8.6	-56
P36	Mauna Loa trail	2745	155.437	19.523		576	394				-10.1	-7.4				-68	-46			-9.0	-59
P37	Mauna Loa trail	3060	155.468	19.533	246	426	279			-8.8	-11.3	-8.3			-60	-79	-52			-10.2	-70
P38	Mauna Loa trail	3340	155.501	19.526	231		317			-9.8		-9.4			-69		-60				
P39	Mauna Loa radio facility	2528	155.457	19.585	340	392[†]	301[†]			-7.4	-10.0[†]	-6.6[†]			-50	-66[†]	-39[†]			-8.7	-56
P40	C. of C. Road, mile 17	24	155.124	19.286	1700	922	251	577	2320	-1.5	-3.9	-1.7	-4.8	-2.2	-7	-23	-2	-29	-9	-2.9	-15
P41	Makaopuhi Crater	876	155.176	19.364		1813[*]	794	2565	1806		-4.9	-2.9	-4.1	-5.2		-28	-9	-21	-28	-4.2	-22
P42A	Kalapana Trail, HVNP	23	155.072	19.320	601					-2.3					-12						
P42B	Kalapana Trail, HVNP	23	155.072	19.320	304					-2.6					-13						
P43	Puu Kalalua	628	155.065	19.407	1512	2355	1314			-3.1	-4.3	-2.6			-13	-21	-4			-3.8	-16
P44	Glenwood Road	695	155.147	19.477	764	1163	786			-3.3	-4.7	-2.4			-14	-26	-2			-4.0	-19
P45A	Pikake Rd., Kurtistown	482	155.079	19.496	1575					-3.3					-15						
P45B	Pikake Rd., Kurtistown	482	155.079	19.496		2532	1892[†]				-4.3	-1.9[†]				-22	-2[†]			-3.6	-16
P46A	Stainback Highway	853	155.193	19.574	1353	2035	2284	2518	3774	-3.4	-4.9	-3.2	-4.5	-4.9	-15	-24	-7	-20	-22	-4.2	-18
P46B	Stainback Highway	853	155.193	19.574	2420					-3.5					-14						
P47	Stainback Highway	1128	155.237	19.562	1074					-3.1					-11						
P48	Stainback Highway	1411	155.278	19.559	1314	909				-4.0	-5.5				-20	-29				-4.6	-24

Site	Location	Elevation (m)	Longitude	Latitude	Precipitation (mm)					$\delta^{18}O$ (‰)					δD (‰)					VWA	
					1	2	3	4	5	1	2	3	4	5	1	2	3	4	5	$\delta^{18}O$	δD
	Saddle Rd., 2000 feet[b]	610																			-6
P49	Gaging Station Waiakea R.	591	155.173	19.640	2559					-3.0					-16						
	Saddle Rd. 2700 feet[b]	823																			-18
P50	Saddle Road	1719	155.371	19.670	759	952	970			-4.4	-7.5	-4.6			-24	-46	-20			-6.1	-34
	Saddle Rd. 5500 feet[b]	1676																			-22
P51	SOH-4 wellpad	369	154.969	19.453	1942	2213	1445	1915	2827	-2.9	-4.1	-2.3	-4.3	-4.1	-11	-19	-3	-20	-19	-3.6	-15
P52	Pahoa	149	154.973	19.540	1811		1226			-2.6		-2.0			-10		-2				
P53	Kurtistown	207	155.049	19.582	1897	1661	1489[†]			-2.7	-3.4	-1.8[†]			-12	-17	-1[†]			-2.8	-12
P54	UH Ag. Exp. Sta., Stainback	186	155.082	19.646	1999	1931	1523			-2.6	-4.0	-2.1			-13	-21	-2			-3.2	-15
P55	Mauna Loa Macadamia Co.	24	155.010	19.660	1484		1104			-2.4		-1.9			-9		-3				
P56	Highway 130 at steam wells	311	154.944	19.470	1564					-2.7					-13						
P57	Highway 132 at Kaniahiku	198	154.913	19.487	1267					-2.5					-8						
P58	Mackenzie State Park	24	154.870	19.441	510	1353	476			-2.1	-3.6	-1.7			-8	-19	-1			-3.2	-15
P59	Cape Kumukahi light	9	154.814	19.518	1033	1441	628	1632	1345	-2.2	-3.7	-1.8	-4.2	-4.9	-9	-19	-2	-20	-29	-3.6	-17
	Club 299 (Hilo airport)[b]	15																			-5
	Hilo, IAEA data[a]	9	155.070	19.720																-2.6	-8

† Oil-type collector, 8-mm layer of silicone oil.
§ Collector overfilled.
* Volume in collector not measured, estimated from surrounding collectors.
‡ Collection interval covers two periods due to difficulty accessing site.
[a] IAEA station 9128500, Hilo, Hawaii, volume-weighted average from 1963, 1967 and 1968 data.
[b] Average value of data from Friedman and Woodcock, 1957, converted to δD relative to VSMOW from δD relative to Lake Michigan standard.
[c] Data from sites P1 and P2 averaged to obtain vwa value.

Appendix 2. Ground water sample locations, average chloride content, and $\delta^{18}O$ and δD content, for the southeast part of the Island of Hawaii. Data from McMurtry et al., 1977 and Tilling and Jones, 1994 are included. Column headings: #: number of samples averaged; Avg. temp.: average temperature measured at time of sampling; Avg. raw: average value unadjusted for seawater content; Avg. adj.: average value of fresh water, seawater component removed; Std.: standard deviation; Dep. hole: depth in meters below sea level to bottom of drillhole; Dep. solid case: depth in meters to bottom of solid casing in well; Init. stat. head: static head in meters above sea level at time well was drilled. Abbreviations: ---: no data available; ng: not given in original database.

ID	State well number	Location description	#	Elev-ation (m)	Long-itude	Lati-tude	Avg. Cl (mg/L)	Avg. temp. (°C)	Avg. raw δD (‰)	Avg. adj. δD (‰)	Std. adj. δD	Avg. raw $\delta^{18}O$ (‰)	Avg. adj. $\delta^{18}O$ (‰)	Std. adj. $\delta^{18}O$	Dep. hole (m)	Dep. solid case (m)	Init. stat. head (m)	Sample method (for wells)
G1		Kaalualu springs	4	0	155.615	18.974	5602	22.1	-20	-29	1.5	-3.5	-5.0	0.12				
G2		Waikapuna spring	1	0	155.582	19.022	4552	---	-18	-24		-3.8	-4.9					
G3	0335-01	Naalehu well	2	227	155.595	19.063	8.3	19.1	-21		1.7	-4.2		0.07	-45.7	-1.2	3.0	pump
G4	0437-01	Waiohinu exploratory well	1	396	155.621	19.073		---	-25			-5.1			91.4		309.7	pump
14		Honuapo mill well[a]	1		155.550	19.092		---	-21			-3.9						pump
G5	0537-01	Haao spring	2	707	155.624	19.091	7.6	18.4	-23		1.5	-4.2		0.03				
G6	0936-01	Mountain House spring	2	1048	155.616	19.158	3.3	16.2	-22		2.0	-4.3		0.04				
G7		Ainapo crack	3	3923	155.580	19.441	0.3	3.0	-78		2.4	-11.2		0.30				
G8		Mauna Loa cabin crack	2	4038	155.585	19.465	0.3	1.0	-88		2.5	-12.3		0.13				
MLS		Mauna Loa summit crack[b]	2	4038				---	-92			-12.5						
G9		Jaggar's cave	2	3974	155.580	19.496	0.6	---	-78		6.8	-11.1		0.92				
G10		Kawa spring	3	2	155.529	19.114	317	18.4	-19	-20	0.5	-4.1	-4.2	0.04				
G11		Punaluu beach spring	3	0	155.508	19.136	502	18.9	-26	-26	0.7	-4.7	-4.8	0.07				
G12	0831-03	Ninole B well	3	7	155.519	19.142	162	18.9	-24	-25	1.3	-4.5	-4.5	0.21	0.6	ng	ng	pump
13		Ninole Springs well[a]	1		155.519	19.142		21.0	-24			-4.6						pump
11		Palima well[a]	1		155.471	19.186		21.0	-42			-6.7					2.7	pump
G13	1229-01	Pahala well	3	339	155.489	19.207	2.9	17.7	-26		1.2	-4.7		0.24	53.0	75.0	116.9	pump
12		Pahala Mill shaft[a]	1		155.480	19.199		---	-31			-5.4					69.5	pump
G14	1331-01	Alili spring	5	902	155.521	19.232	3.9	17.2	-24		1.0	-4.6		0.06				

ID	State well number	Location description	#	Elev-ation (m)	Long-itude	Lati-tude	Avg. Cl (mg/L)	Avg. temp. (°C)	Avg. raw δD (‰)	Avg. adj. δD (‰)	Std. adj. δD	Avg. raw $\delta^{18}O$ (‰)	Avg. adj. $\delta^{18}O$ (‰)	Std. adj. $\delta^{18}O$	Dep. hole (m)	Dep. solid case (m)	Init. stat. head (m)	Sample method (for wells)
G15		Crack near Kamehame hill	5	6	155.484	19.143	705	19.0	-31	-32	2.0	-5.2	-5.4	0.19				
G16		Waioala spring	3	0	155.453	19.153	871	19.0	-36	-38	1.0	-5.9	-6.2	0.14				
G17		Pueo spring	3	0	155.446	19.160	485	20.3	-39	-40	2.3	-6.1	-6.3	0.21				
G18		Waiapele crack	3	6	155.439	19.165	581	21.3	-39	-40	1.8	-6.0	-6.1	0.15				
G19		Puu Elemakule spring	3	0	155.333	19.240	9480	39.1	-17	-34	4.2	-2.4	-4.7	0.20				
G20		Opihinehe spring	1	0	155.324	19.245	4961	37.0	-25	-34		-4.1	-5.5					
G21	2317-01	Kilauea summit borehole	2	1099	155.289	19.396	4.1	34.3	-32			-5.6		0.06	-158.8	786.7	550.4	dip
32		Kilauea summit borehole[a]	2	1099				79.0	-30			-4.7						dip
KBW		Kilauea summit borehole[b]	9	1099				---	-28			-4.6						
WR		Wright Road wells[b]	2					---	-21			-4.6						
G22		Kaaha cracks	5	6	155.303	19.265	1787	27.9	-29	-32	0.9	-4.6	-5.1	0.12				
G23		Kalue crack	2	0	155.289	19.268	1824	24.0	-28	-30	0.6	-4.6	-5.1	0.03				
G24		Halape springs	4	5	155.258	19.274	2766	26.9	-24	-28	0.7	-4.1	-4.8	0.12				
G25		Keauhou beach spring	1	0	155.236	19.269	1785	27.0	-27	-30		-4.5	-4.9					
G26		Apua point crack	3	8	155.198	19.263	1802	22.5	-22	-24	2.9	-4.0	-4.4	0.15				
G27		Crack near Kaena Point	3	0	155.129	19.280	2241	25.0	-21	-24	0.6	-3.9	-4.4	0.02				
8	2102-01	Pulama well[a]	1		155.038	19.354		28.0	-21			-4.0						dip
G28		Waiakea stream at gauge	3	591	155.175	19.642	1.9	19.2	-15		0.5	-3.5		0.04				
G29	4211-01	Olaa Flume spring	1	603	155.188	19.700	22	17.6	-15			-3.6						
G30	3603-01	Olaa well #3	1	177	155.054	19.609	3.1	19.6	-17			-3.6			ng	ng	ng	pump
G31	3804-01	Keaau (Shipman) well	3	168	155.071	19.637	1.7	18.7	-21		3.2	-4.4		0.29	-44.5	-30.2	10.0	pump
G32	3802-03	Olaa #1 (Keaau Mill 1)	1		155.034	19.634	2.4	19.0	-19			-4.2						pump
27		Olaa mill well[a]	1		155.035	19.636		22.0	-20			-3.9						pump
PSM		Puna Sugar Mill, Olaa[b]	1					---	-18			-3.8						
G33		Waiakea Pond	1	0	155.076	19.721	1223	21.0	-12	-13		-3.5	-3.7					
26		Hilo Electric well[a]	1		155.064	19.708		24.0	-15			-3.3						pump

ID	State well number	Location description	#	Elev-ation (m)	Long-itude	Lati-tude	Avg. Cl (mg/L)	Avg. temp. (°C)	Avg. raw δD (‰)	Avg. adj. δD (‰)	Std. adj. δD	Avg. raw $\delta^{18}O$ (‰)	Avg. adj. $\delta^{18}O$ (‰)	Std. adj. $\delta^{18}O$	Dep. hole (m)	Dep. solid case (m)	Init. stat. head (m)	Sample method (for wells)
G34		Haena beach spring	3	1	154.986	19.647	287	19.1	-20	-21	2.0	-4.0	-4.1	0.19				
G35	3588-01	Paradise Park well	2	44	154.976	19.596	80	20.3	-14		0.2	-3.5		0.13	-7.0	2.1	2.4	dip
G36	2487-01	Keauohana well	3	229	154.955	19.416	92	24.6	-15		1.3	-3.3		0.15	-15.2	1.5	0.9	pump
6		Keauohana well[a]	1					24.0	-16			-3.4						pump
G37	3185-01	Hawaiian Beaches well	3	123	154.933	19.520	12	22.0	-14		1.2	-3.3		0.20	-13.4	-7.3	3.2	pump
G38	2986-01	Pahoa 2A well	3	215	154.946	19.490	4.5	23.7	-15		0.8	-3.6		0.14	-15.2	7.0	5.4	pump
4		Pahoa well 2[a]	1					23.0	-18			-3.8						pump
3		Kapoho landing strip well[a]	3		154.873	19.508		34.0	-14			-3.1						dip
G39	3188-01	Keonepoko Nui well	3	184	154.968	19.518	3.5	20.2	-20		2.6	-4.0		0.33	-14.3	0.6	4.6	pump
9		Allison well[a]	1		154.853	19.472		38.0	-17			-3.3						dip
10		Malama-Ki well[a]	3		154.883	19.458		54.3	-9			-1.6						dip
G40	2983-01	PGV MW-1 well	2	186	154.894	19.486	18	42.8	-12		0.8	-3.0		0.07	-33.5	-3.7	2.4	
G41	2883-07	PGV MW-2 well	3	179	154.892	19.477	810	60.3	-11	-11	0.6	-2.7	-2.8	0.09	-15.8	4.3	5.7	
G42	2983-02	PGV MW-3 well	1	186	154.894	19.486	20	44.0	-11			-3.1			-33.5	-21.3	4.9	
G43	3080-01	Kapoho Crater well	3	12	154.839	19.504	145	25.5	-16	-16	1.4	-3.3	-3.4	0.25	-2.4	-2.4	1.0	pump
5		Kapoho Cone shaft[a]	1		154.839	19.506		25.0	-19			-3.6						dip
G44		Pohoiki spring	3	1	154.846	19.461	3798	34.7	-10	-13	2.3	-2.5	-3.1	0.13				
1		Pohoiki spring[a]	1					35.0	-14			-2.7						
2		Allison spring[a]	1		154.839	19.465		31.0	-12			-2.2						
G45		Campbell spring	1	5	154.838	19.467	3505	37.4	-11	-13		-2.3	-2.8					
G46		Pualaa Park spring	2	0	154.834	19.472	5324	35.3	-10	-13	0.2	-2.4	-3.3	0.01				
G47		Kapoho Beachlots pond	3	3	154.825	19.492	2752	32.8	-12	-14	1.7	-2.6	-3.1	0.29				
G48		Vacationland pond	1	0	154.825	19.494	2168	31.5	-14	-16		-2.5	-2.8					
G49		Lighthouse spring	4	1	154.809	19.521	1956	28.6	-12	-14	1.7	-2.9	-3.3	0.22				
G50		Orr's spring	1	0	154.824	19.529	944	22.0	-15	-16		-3.5	-3.7					
G51	2982-01	GTW-3 well	1	172	154.882	19.487	6042	89.4	-7	-10		-1.8	-2.6		-38.7	ng	ng	

ID	State well number	Location description	#	Elev-ation (m)	Long-itude	Lati-tude	Avg. Cl (mg/L)	Avg. temp. (°C)	Avg. raw δD (‰)	Avg. adj. δD (‰)	Std. adj. δD	Avg. raw $\delta^{18}O$ (‰)	Avg. adj. $\delta^{18}O$ (‰)	Std. adj. $\delta^{18}O$	Dep. hole (m)	Dep. solid case (m)	Init. stat. head (m)	Sample method (for wells)
31		Geothermal test hole 3[a]	4					90.5	-12			-2.5						
G52	ng	KS-9 well[c]	1	ng	154.896	19.480	2.1	207.0	-1			+0.2			ng	ng	ng	
G53	ng	KS-10 well[c]	1	ng	154.896	19.480	14040	205.0	-6			-0.7			ng	ng	ng	
		Pohoiki seawater			154.845	19.460	17440	---	1			0.4						
		Pohoiki seawater					18135	---	3			0.1						
		South Point seawater					18340	26.0	1			0.1						

[a]Data from McMurtry et al., 1977.
[b]Data from Tilling and Jones, 1995.
[c]Isotopes were analyzed for separated brine, reported temperature is temperature of separation, steam data not presently available.